

THE MOLECULAR WEIGHT DEPENDENCE  
OF INTRINSIC VISCOSITY

By

JOHN D. MORRISON

Bachelor of Science

Oklahoma Christian College

Oklahoma City, Oklahoma

1965

Submitted to the Faculty of the Graduate College  
of the Oklahoma State University  
in partial fulfillment of the requirements  
for the Degree of  
MASTER OF SCIENCE  
July, 1968

OKLAHOMA  
STATE UNIVERSITY  
LIBRARY

JAN 30 1969

THE MOLECULAR WEIGHT DEPENDENCE  
OF INTRINSIC VISCOSITY

Thesis Approved:

*G. B. Hurston*

Thesis Adviser

*E. G. Kolb*

*N. N. Durham*

Dean of the Graduate College

696397

#### ACKNOWLEDGMENTS

The author wishes to express his gratitude to Dr. G. B. Thurston for his constant encouragement and valuable advice during the investigations reported in this work; to Miss Rita Payne for her assistance in the preparation of the manuscript; and to the U. S. Army Research Office, Durham, for a grant awarded to Dr. Thurston for the financial support of this work.

## TABLE OF CONTENTS

Chapter	Page
I. INTRODUCTION . . . . .	1
II. THEORY . . . . .	5
The Forces Acting on the Model . . . . .	5
The Hydrodynamic Interaction Tensor . . . . .	10
The Diffusion Equation and Normal Coordinates . . . . .	22
The Application of the Eigenvalues to the Intrinsic Viscosity . . . . .	38
The Calculation of Relaxation Times From Intrinsic Viscosity Data . . . . .	40
III. NUMERICAL EIGENVALUE CALCULATIONS AND RELATED FUNCTIONS . .	42
Preliminary Calculations . . . . .	42
Eigenvalue Calculations . . . . .	47
Calculation of Eigenvalue Dependent Functions . . . . .	63
IV. COMPARISON WITH MEASUREMENTS . . . . .	76
Polystyrene in Aroclor 1248 . . . . .	76
Other Intrinsic Viscosity Measurements and Conclusions . . . . .	88

# LIST OF TABLES

Table	Page
I. Comparison of Kirkwood-Riseman and Treloar Values for $\langle \frac{1}{R_{jk}} \rangle$ . . . . .	48
II. Free-draining Eigenvalues . . . . .	49
III. Treloar Eigenvalues . . . . .	50
IV. Kirkwood-Riseman Eigenvalues . . . . .	52

# LIST OF FIGURES

Figure	Page
1. $\lambda_p$ Versus $N$ for the Free-draining Case . . . . .	56
2. Pyun and Fixman Values of $\lambda_p$ Versus $N$ for $h^*=0.1$ . . . . .	58
3. Treloar Values of $\lambda_p$ Versus $N$ for $h^*=0.1$ . . . . .	60
4. Kirkwood-Riseman Values of $\lambda_p$ Versus $N$ for $h^*=0.1$ . . . . .	62
5. $\phi N^{1/2}$ Versus $N$ Using Treloar Eigenvalues . . . . .	66
6. $\phi N^{1/2}$ Versus $N$ Using Kirkwood-Riseman Eigenvalues . . . . .	68
7. $\phi N^{1/2}$ Versus $N$ Using Pyun and Fixman Eigenvalues . . . . .	70
8. $C(N, h^*)$ Versus $N$ Using Kirkwood-Riseman Eigenvalues . . . . .	72
9. Comparison of $C(N, h^*)$ Versus $N$ Calculated From Kirkwood-Riseman and Pyun and Fixman Eigenvalues . . . . .	74
10. $[\eta]$ Versus $M$ For Polystyrene in Aroclor 1248 . . . . .	83
11. $\tau_1$ Versus $M$ Calculated From Intrinsic Viscosity . . . . .	85
12. Curves for $\tau_1'(c)$ , $\tau_1'(c)/K(c)$ , and $\tau_1$ Versus $M$ From Oscillatory Flow Birefringence Measurements. $\tau_1$ Versus $M$ From Intrinsic Viscosity Measurements . . . . .	87
13. $[\eta]$ Versus $M$ for Polystyrene Solutions in Benzene (39), Decalin, Dioctylphthalate, and Toluene (40) . . . . .	90
14. $[\eta]$ Versus $M$ for Poly- $\gamma$ -benzyl- L -glutamate (45), Poly $\alpha$ -Methylstyrene (46), and Polyoxyethyleneglycol (47) . . . . .	92

## CHAPTER I

### INTRODUCTION

Much of the mathematical theory describing polymers in solution stems from the work of Werner Kuhn. Kuhn and his coworkers (1), assuming that the polymer molecules take the shape of a very loose coil when dissolved in certain solvents, introduced the concept of a "statistical chain element" made up of a number of monomer units and constituting a portion of the chain of end-to-end length  $b$ . This length of the statistical chain element is taken such that when proceeding along the polymer chain, the orientation of a given statistical chain element is independent of the orientation of the neighboring statistical segments. The length of the statistical segment would thus be different for different polymers, depending on the angle formed by two successive valence directions along the polymer backbone and the degree of freedom of each bond. A key point in the Kuhn theory was that the polymer subchain that forms the statistical segment has a preferred end-to-end distance that can be found from purely statistical considerations (2, 3). Kuhn proposed that, just as with the case of the entire polymer, the ends of each statistical segment tend to assume a random distribution as a consequence of thermal diffusion, with the result that an effective force of magnitude  $\frac{3 k T h}{b^2}$  is exerted on the segment ends when the segment is stretched, where  $k$  is Boltzmann's constant,  $T$  is the absolute temperature,  $h$  is the end-to-end

distance of the segment or subchain, and  $b$  is the rms or "preferred" segment length. This allows each segment to be treated as a Hookean spring. Kuhn and Kuhn (1) included both internal viscosity to explain energy losses within the chain, and a variable draining condition, while Kuhn and Gr $\ddot{u}$ n (4) used the polarizability of each statistical segment to explain some birefringence effects.

Other workers used the statistical segment idea of Kuhn to form models of a real polymer. Kramers (5) examined the "pearl necklace" model, in which he replaced the polymer with a number of beads connected by massless linking rods. He assumed that the solvent could exert forces on the chain only at the beads and also included interaction effects between the beads. Hermans (6) also investigated the effect of hydrodynamic interaction between the beads of the chain, as did Kirkwood and Riseman (7).

Rouse (8) and Bueche (9) working independently characterized the polymer as a number of beads connected by massless Hookean springs whose force constant is given by  $\frac{3kT}{b^2}$ , from the Kuhn theory, and where each of the springs corresponds to one of the Kuhn statistical segments. Thus the model has  $N$  identical segments joining  $N+1$  identical beads, with perfect freedom in each joint, as follows from the independence of the orientation of the statistical segments. Both Rouse and Bueche adopted a coordinate transformation to normal coordinates, which allowed much of the mathematics to be cast in a simpler matrix form.

Zimm (10, 11), Cerf (12, 13), and Peterlin (14, 15) have done extensive work based on the model of Rouse and Bueche. Zimm did not include internal viscosity in his treatment, while Cerf did, although he did not solve for time dependent effects.



The above work was accompanied with the mathematical assumption that  $N$ , the number of statistical segments, was quite large. Recent research by Thurston and Schrag (16) have indicated a direct proportionality between  $N$  and  $M$ , the molecular weight. Data from oscillatory flow birefringence experiments have indicated only a finite number of relaxation times associated with polymer stress, which is to be expected with a finite value of  $N$  required by a direct  $M, N$  proportionality for a given polymer.

The work of Thurston and Peterlin (17) used a set of eigenvalues  $\lambda_p$  to predict theoretical curves for intrinsic viscosity and oscillatory flow birefringence. In this work  $h^*$ , a segmental hydrodynamic interaction factor,  $\psi/f$ , the ratio of the internal viscosity coefficient to the segmental friction factor, and  $N$ , the number of statistical segments were used as significant parameters of the theory. The eigenvalues, however, were computed by a method developed by Pyun and Fixman (18) which assumed that  $N$  was large and  $\rho$  was small compared to  $N$ . This resulted in marked deviation of the theoretical predictions from experimental values for intrinsic viscosity and birefringence for low molecular weight (i.e., for low  $N$ ) samples (19).

Quite different mathematical models have been proposed by other workers. The persistent chain theory of Gotlib and Svetlov (20) predicts the observed molecular weight dependence of intrinsic viscosity and birefringence for low molecular weights by the use of a persistence length measured along the polymer chain. On the assumption that the portion of the solvent contained within the coiled polymer chain should be practically immobilized and forced to move with the polymer, several models have been advanced which replace the polymer coil and its

contained solvent with an equivalent particle. Sadron (21, 22) has proposed the equivalent ellipsoid (which approaches a sphere for high molecular weights) and Flory has proposed an equivalent sphere model (23), which can be swelled or compressed by placing the polymer in different solvents (24). The major difficulty in the persistent chain theory and the equivalent particle models, however, is the inability to predict the plurality of relaxation times observed in oscillatory flow birefringence. In addition, the equivalent particle models yield no conceptual information about the structure of the polymer itself.

The object of this paper is to compute exact values for the set of eigenvalues  $\lambda_\rho$  for small values of  $N$ , and hence for low molecular weight polymers and to compare the predicted relation between intrinsic viscosity and molecular weight with experimental measurements. This is done following the method described by Thurston (25) in which the approximate eigenvalues of Pyun and Fixman were used. In addition, the molecular weight dependence of the terminal (longest) relaxation time of the chain obtained from intrinsic viscosity measurements under steady flow conditions is compared with that from independent measurements of oscillatory flow birefringence.

## CHAPTER II

### THEORY

#### The Forces Acting on the Model

The model to be used to describe a long chain polymer consists of  $N$  statistical segments joining  $N+1$  beads, numbered from  $i = 0$  to  $i = N$ . The entire model is assumed to be suspended in a viscous solvent of viscosity  $\eta_s$  which can interact with the chain through the beads only. Following Kuhn, the assumption is made that the beads tend to assume a random distribution due to thermal motion (diffusion) and that each statistical segment has a length  $b$  which responds to stretching as if it were a Hookean spring of spring constant  $\frac{3kT}{b^2}$ , where  $k$  is Boltzmann's constant, and  $T$  is the absolute temperature (1). If now the position of the  $i$ -th bead is denoted by  $(x_i, y_i, z_i)$ , then the components of the spring force acting on the  $i$ -th bead can be given by

$$F_{x_i}^{sp} = (-3kT/b^2)[-x_{i-1} + 2x_i - x_{i+1}]. \quad (\text{II-1})$$

Following the formalism of Cerf (13), the notation can be considerably reduced if a matrix form is adopted. Working with  $x$ -components only, introduce the column vectors

$$\vec{x} = \begin{pmatrix} x_0 \\ x_1 \\ \vdots \\ x_N \end{pmatrix} \quad \text{and} \quad \vec{F}_x^{sp} = \begin{pmatrix} F_{x_0}^{sp} \\ F_{x_1}^{sp} \\ \vdots \\ F_{x_N}^{sp} \end{pmatrix}, \quad (\text{II-2})$$

where  $\chi_i$  is the  $\chi$ -component of bead  $i$  and  $F_{\chi_i}^{sp}$  is the  $\chi$ -component of the spring force acting on bead  $i$ . Equation (II-1) can be written for all the beads as

$$\begin{aligned} F_{\chi_0}^{sp} &= -\frac{3kT}{b^2} [\chi_0 - \chi_1], \\ F_{\chi_1}^{sp} &= -\frac{3kT}{b^2} [-\chi_0 + 2\chi_1 - \chi_2], \\ F_{\chi_2}^{sp} &= -\frac{3kT}{b^2} [-\chi_1 + 2\chi_2 - \chi_3], \\ &\vdots \\ F_{\chi_N}^{sp} &= -\frac{3kT}{b^2} [-\chi_{N-1} + \chi_N]. \end{aligned} \quad (\text{II-3})$$

Apply the boundary conditions that  $\chi_{-1} = \chi_0$  and  $\chi_N = \chi_{N+1}$ .

These are necessary for equation (II-1) to hold for every bead. Using the vectors  $\vec{F}^{sp}$  and  $\vec{\chi}$ , equation (II-3) can be written as

$$\vec{F}^{sp} = -\frac{3kT}{b^2} \begin{pmatrix} 1 & -1 & 0 & \cdots & 0 & 0 \\ -1 & 2 & -1 & & 0 & 0 \\ 0 & -1 & 2 & & 0 & 0 \\ \vdots & & & & & \\ 0 & 0 & 0 & & 2 & -1 \\ 0 & 0 & 0 & & -1 & 1 \end{pmatrix} \begin{pmatrix} \chi_0 \\ \chi_1 \\ \chi_2 \\ \vdots \\ \chi_{N-1} \\ \chi_N \end{pmatrix}, \quad (\text{II-4})$$

or

$$\vec{F}^{sp} = -\frac{3kT}{b^2} \mathbb{A} \cdot \vec{\chi}, \quad (\text{II-5})$$

where

$$\mathbb{A} = \begin{pmatrix} +1 & -1 & 0 & \cdots & 0 & 0 \\ -1 & 2 & -1 & & 0 & 0 \\ 0 & -1 & 2 & & 0 & 0 \\ \vdots & & & & & \\ 0 & 0 & 0 & & 2 & -1 \\ 0 & 0 & 0 & & -1 & 1 \end{pmatrix}. \quad (\text{II-6})$$

A force of internal viscosity is considered to act on each bead and is given in matrix form as

$$\vec{F}^{\text{int vis}} = -\mathcal{F}(\vec{\dot{\chi}} - \vec{\dot{\chi}}_{\Omega}), \quad (\text{II-7})$$

where

$$\vec{\dot{\chi}} = \begin{pmatrix} \dot{\chi}_0 \\ \dot{\chi}_1 \\ \vdots \\ \dot{\chi}_N \end{pmatrix} \quad (\text{II-8})$$

and

$$\vec{\dot{\chi}}_{\Omega} = \begin{pmatrix} \dot{\chi}_{\Omega 0} \\ \dot{\chi}_{\Omega 1} \\ \vdots \\ \dot{\chi}_{\Omega N} \end{pmatrix}. \quad (\text{II-9})$$

The components of  $\vec{\dot{\chi}}$  are the  $\chi$ -velocity components of the  $N+1$  beads and the components of  $\vec{\dot{\chi}}_{\Omega}$  are the  $\chi$ -components of the velocity of rotation due to the velocity of the fluid. The form of the internal viscosity is due to Cerf and is also used by Peterlin (26). The matrix  $\mathcal{F}$  will be explained in more detail later.

The solvent is assumed to interact with the chain only at the beads in an expression of the type of Stokes' law. That is, the component of the force exerted on the  $i$ -th bead due to the viscosity of the solvent is taken to be of the form

$$F_{\chi_i} = -f(\dot{\chi}_i - \dot{\chi}_{\ell,i}), \quad (\text{II-10})$$

where  $f$  is a friction constant. In matrix notation this equation

may be written as

$$\vec{F}_\chi = -f(\vec{\chi} - \vec{\chi}_d), \quad (\text{II-11})$$

where  $\vec{\chi}$  refers to the  $\chi$ -velocities of the individual beads, and  $\vec{\chi}_d$  refers to the  $\chi$ -components of the solvent velocity at the location of each bead if the bead were not present.

In addition to the spring force, and that due to solvent viscosity, an effective force is assumed to act on each bead to account for Brownian motion. This force of diffusion, denoted in the matrix notation as the column vector  $\vec{F}_\chi''$ , is a function of the distribution function  $\Psi$  of the system.  $\Psi(\chi_0, y_0, \dots, z_N)$  is a function of all the coordinates such that  $\Psi$  is the probability of finding each bead  $i$  with position coordinates between  $\chi_i$  and  $\chi_i + d\chi_i$ , between  $y_i$  and  $y_i + dy_i$ , and between  $z_i$  and  $z_i + dz_i$ . According to the theory of Brownian motion (10, 27) the  $\chi$ -component of the effective diffusion force acting on the  $i$ -th bead is

$$F_{\chi_i}'' = -kT \frac{\partial \ln \Psi}{\partial \chi_i}. \quad (\text{II-12})$$

In matrix form this can be written for the  $N+1$  beads as

$$\vec{F}_\chi'' = -kT \vec{\nabla}_\chi \ln \Psi, \quad (\text{II-13})$$

where  $k$  is Boltzmann's constant,  $T$  is the absolute temperature, and  $\vec{\nabla}_\chi$  is the operator denoted by the column vector

$$\vec{\nabla}_\chi = \begin{pmatrix} \partial/\partial \chi_0 \\ \partial/\partial \chi_1 \\ \vdots \\ \partial/\partial \chi_N \end{pmatrix}. \quad (\text{II-14})$$

Assuming that the solvent viscosity is great enough, the inertial effects may be neglected and the force equation of the  $i$ -th bead may be written in matrix form as the sum of the forces just described, or

$$-\frac{3kT}{b^2} A \cdot \vec{r} - \mathcal{H}(\vec{r} - \vec{r}_R) - f(\vec{r} - \vec{r}_s) - kT \vec{\nabla}_s \ln \psi = 0. \quad (\text{II-15})$$

The excluded volume effect that has been considered by Peterlin (28) and others (29) has not been included here since it has application for polymers of high molecular weight (and thus a large number of statistical segments), and its effect upon low molecular weight polymers is negligible.

Equation (II-15) can be expanded and partially solved for  $\vec{r}$ .

Then

$$\vec{r} = \vec{r}_s + f^{-1} \left[ -\frac{3kT}{b^2} A \cdot \vec{r} - \mathcal{H}(\vec{r} - \vec{r}_R) - kT \vec{\nabla}_s \ln \psi \right]. \quad (\text{II-16})$$

The determination of  $\vec{r}_s$ , the  $s$ -components of the solvent velocity at the site of each bead if that bead were removed, is complicated by the fact that the presence of the rest of the chain perturbs the motion of the solvent at the site of each bead. To account for this hydrodynamic interaction, Kirkwood and Riseman (7) used the quasi-static velocity perturbation expressions of Oseen as given by Burgers (30) to obtain the perturbation  $\vec{v}'$  at a point  $\vec{R}_s$  from the locus of application of a force  $\vec{F}_s$  on the solvent in the form

$$\vec{v}'(\vec{R}_s) = \Pi(\vec{R}_s) \cdot \vec{F}_s, \quad (\text{II-17})$$

where the matrix  $\Pi$  is given in dyadic form by

$$\Pi(\vec{R}_\ell) = \frac{1}{8\pi\eta_s R_\ell} \left\{ \vec{1} + \frac{\vec{R}_\ell \vec{R}_\ell}{R_\ell^2} \right\}, \quad (\text{II-18})$$

where  $\eta_s$  is the solvent viscosity. Since the motion of the solvent at the site of the  $i$ -th bead is the sum of the unperturbed velocity  $\vec{\dot{\chi}}_{\ell,i}^0$  and the perturbing velocity  $\vec{V}_i'$  due to the presence of the other beads in the chain,  $\vec{\dot{\chi}}_{\ell,i}$  can be written in matrix form as

$$\vec{\dot{\chi}}_\ell = \vec{\dot{\chi}}_\ell^0 - \Pi \cdot \vec{F}_\chi, \quad (\text{II-19})$$

where  $\vec{F}_\chi$  is the force exerted by the solvent on the bead as given by (II-11).

### The Hydrodynamic Interaction Tensor

Since the exact locations of the beads are unknown, the space-average values of the hydrodynamic interaction tensor  $\Pi$  are used, denoted by  $\langle T_{jk} \rangle$ . The indices  $j$  and  $k$  refer to the indices of the two beads related by that tensor element. This average value is found in the following way. Burgers (30), using the quasi-static velocity perturbation expressions of Oseen, gives the components of the perturbing velocity at a point  $x, y, z$  due to a force  $\vec{F}^\ell = (F_x^\ell, F_y^\ell, F_z^\ell)$  located at the origin as

$$v_{\chi_i} = \frac{1}{8\pi\eta_s R} \left[ F_{\chi_i}^\ell + \frac{\chi_i}{R^2} \sum_{i=1}^3 \chi_i F_{\chi_i}^\ell \right], \quad (\text{II-20})$$

where  $\chi_1 = x, \chi_2 = y, \chi_3 = z$ , (II-21)

and  $R = [x^2 + y^2 + z^2]^{1/2}$ . (II-22)

When the diffusion equation is solved a bit later, the motion applied to the solvent will be of the type



$$\begin{aligned}
\dot{x}_{li}^0 &= G z_i \\
\dot{y}_{li}^0 &= 0 \\
\dot{z}_{li}^0 &= 0,
\end{aligned}
\tag{II-23}$$

where  $G$  is the velocity gradient in the  $z$  direction. In general  $G$  may be complex. With the problem stated in this way, a bead of the chain will move primarily in the  $x$  direction and only very slightly in the  $z$  direction (due to a small rotation), with the result that the force exerted on the solvent by the bead has only an  $x$ -component of significance for this level of treatment. With these assumptions, the  $x$ -component of equation (II-20) may be written as

$$\begin{aligned}
v_x &= \frac{1}{8\pi\eta_s R} \left[ F_x^l + \frac{x}{R^2} \cdot F_x^l \right] \\
&= \frac{1}{8\pi\eta_s R} \left[ 1 + \frac{x^2}{R^2} \right] F_x^l.
\end{aligned}
\tag{II-24}$$

On the average, the projected value of  $R$  on any axis (in this case the  $x$ -axis) is zero. But the average squared value of the projection is  $\frac{R^2}{3}$  (31). That is,

$$\overline{x^2} = \frac{R^2}{3}.
\tag{II-25}$$

Then

$$\begin{aligned}
\left[ 1 + \frac{\overline{x^2}}{R^2} \right] &= \left[ 1 + \frac{R^2}{3R^2} \right] \\
&= 4/3.
\end{aligned}
\tag{II-26}$$

Thus, on the average,

$$\begin{aligned}
v_x &= \left\langle \frac{1}{8\pi\eta_s} \cdot \frac{1}{R} \cdot \frac{4}{3} \right\rangle F_x \\
&= \frac{1}{6\pi\eta_s} \left\langle \frac{1}{R} \right\rangle F_x.
\end{aligned}
\tag{II-27}$$

Applying this to the effect of the motion of bead  $k$  upon bead  $j$ , bead  $k$  can be considered as at the origin of the previous discussion and the magnitude of the vector connecting the two as  $R_{jk}$ . Then  $v_x$  is the perturbing velocity of the solvent at bead  $j$  due to bead  $k$  and can be written as

$$v_x = \frac{1}{6\pi\eta_s} \left\langle \frac{1}{R_{jk}} \right\rangle F_{v_k}. \quad (\text{II-28})$$

Since the total perturbing velocity of the solvent at the site of bead  $j$  is the sum of the effects of all the beads as given by equation (II-17), the perturbed solvent velocity at  $j$  is given as

$$\begin{aligned} \dot{\gamma}_{lj}^0 &= \pi(\vec{R}) \cdot \vec{F}^l \\ &= \sum_{\substack{k=0 \\ k \neq j}}^N T_{jk} \cdot F_k^l. \end{aligned} \quad (\text{II-29})$$

Then, comparing (II-29) and (II-28),  $\langle T_{jk} \rangle$  can be written as

$$\langle T_{jk} \rangle = \frac{1}{6\pi\eta_s} \left\langle \frac{1}{R_{jk}} \right\rangle, \quad (\text{II-30})$$

where  $\left\langle \frac{1}{R_{jk}} \right\rangle$  is the average value of the reciprocal of the distance from bead  $j$  to bead  $k$ .

The determination of the above distances and averages depends upon the precise interpretation that is made of the nature of the statistical segments. If one takes all  $N$  segments to be of fixed length  $b$ , then the problem of finding the distribution function of  $R_{jk}$  is the same as the problem of finding the distribution function of the displacement vector after a three-dimensional random walk of  $|j-k|$  steps, each step being the same fixed length. If, however, one assumes the length of the statistical segments to be distributed in a Gaussian

manner with a root mean square length of  $b$ , the problem still reduces to the previous random walk, but one with steps having a Gaussian distribution of length. For steps of fixed length  $b$ , the probability

$W_z(\vec{R}) d\vec{R}$  that the displacement  $\vec{R}$  will be in the interval  $(\vec{R}, \vec{R} + d\vec{R})$  after  $Z$  displacements is given by

$$W_z(\vec{R}) = \frac{1}{2\pi^2 |\vec{R}|} \left[ \int_0^\infty \sin(|\vec{\rho}| |\vec{R}|) \cdot \left\{ \frac{\sin(|\vec{\rho}| b)}{|\vec{\rho}| b} \right\}^Z \cdot |\vec{\rho}| d|\vec{\rho}| \right], \quad (\text{II-31})$$

where  $|\vec{\rho}|$  is a dummy variable and  $b$  is the fixed segment (step) length (31, 32). This distribution function, due to Rayleigh (33), is tedious to use in calculations. Another form of this distribution function is due to Treloar (31) and is easier to use. Treloar's distribution function is of the form

$$W_z(\vec{R}) = \frac{1}{8\pi b^2 R} \cdot \frac{Z^{Z-2}}{(Z-2)!} \sum_{s=0}^k (-1)^s \frac{Z!}{s!(Z-s)!} \left(m - \frac{s}{Z}\right)^{Z-2}, \quad (\text{II-32})$$

where

$$m = \frac{1}{2} \left( 1 - \frac{R}{Zb} \right), \quad (\text{II-33})$$

and the upper limit of the summation  $k$  is determined by the condition

$$k \leq mZ \leq k+1, \quad (\text{II-34})$$

One may note that  $W(\vec{R})$  automatically goes to zero for  $R > Zb$ , since in that case  $m < 0$  and  $k < 0$ .

In order to illustrate the use of the Treloar distribution function, the case for  $Z = 3$  will be worked in detail. For  $Z = 3$ ,

by equation (II-33)

$$m = \frac{1}{2} \left( 1 - \frac{R}{3b} \right). \quad (\text{II-35})$$

Thus

$$mZ = \frac{3}{2} \left( 1 - \frac{R}{3b} \right) = \frac{3}{2} - \frac{1}{2} \left( \frac{R}{b} \right). \quad (\text{II-36})$$

From this the values of  $k$  are found to be

$$\begin{aligned} k &= 0, & b < R < 3b, \\ k &= 1, & 0 < R < b. \end{aligned} \quad (\text{II-37})$$

For  $k=0$ ,  $W(\vec{R})$  is given by

$$W(\vec{R}) = \frac{1}{8\pi b^2 R} \frac{3}{1!} \frac{1}{2} \left( 1 - \frac{R}{3b} \right),$$

or

$$W(\vec{R}) = \frac{1}{16\pi b^3 R} (3b - R), \quad (\text{II-38})$$

for  $b < R < 3b$ .

For  $k=1$ ,  $W(\vec{R})$  is given by

$$W(\vec{R}) = \frac{1}{8\pi b^2 R} \frac{3!}{1!} \left\{ \frac{1}{2} \left( 1 - \frac{R}{3b} \right) - 3 \left[ \frac{1}{2} \left( 1 - \frac{R}{3b} \right) - \frac{1}{3} \right] \right\}$$

or

$$W(\vec{R}) = \frac{1}{8\pi b^2}, \quad (\text{II-39})$$

for  $0 < R < b$ .

As before,  $W(\vec{R}) = 0$  for  $R > 3b$ .

The distribution function needed to calculate the averages in equation (II-30) is not  $W(\vec{R})$ , however, but  $W(R)$ . These are related by the expression

$$\begin{aligned} W(R) dR &= \int_{\theta} \int_{\psi} W(\vec{R}) dR \cdot R^2 \sin \theta d\theta d\psi \\ &= 4\pi R^2 W(\vec{R}) dR. \end{aligned} \quad (\text{II-40})$$

Thus

$$W(R) = 4\pi R^2 W(\vec{R}). \quad (\text{II-41})$$

Expressions for  $W(R)$  for  $Z=2$  through  $Z=6$  are given below:

$$\begin{aligned} Z=2: \\ W(R) &= \frac{R}{2b^2}, \quad 0 < R < 2b; \end{aligned} \quad (\text{II-42})$$

$$\begin{aligned} Z=3: \\ W(R) &= \frac{R^2}{2b^2}, \quad 0 < R < b, \\ W(R) &= \frac{3R}{4b^2} - \frac{R^2}{4b^2}, \quad b < R < 3b; \end{aligned} \quad (\text{II-43})$$

$$\begin{aligned} Z=4: \\ W(R) &= \frac{R^2}{2b^2} - \frac{3R^3}{16b^4}, \quad 0 < R < 2b, \\ W(R) &= \frac{R}{b^2} - \frac{R^2}{2b^3} + \frac{R^3}{16b^4}, \quad 2b < R < 4b; \end{aligned} \quad (\text{II-44})$$

$$\begin{aligned} Z=5 \\ W(R) &= \frac{1}{96} \left[ \frac{30R^2}{b^3} - \frac{6R^4}{b^5} \right], \quad 0 < R < b, \\ W(R) &= \frac{1}{96} \left[ -\frac{10R}{b^2} + \frac{60R^2}{b^3} \right. \\ &\quad \left. - \frac{30R^3}{b^4} + \frac{4R^4}{b^5} \right], \quad b < R < 3b, \end{aligned} \quad (\text{II-45})$$

$$W(R) = \frac{1}{96} \left[ \frac{125R}{b^2} - \frac{75R^2}{b^3} + \frac{15R^3}{b^4} - \frac{R^4}{b^5} \right], \quad (II-45)$$

$$3b < R < 5b;$$

$$Z = 6:$$

$$W(R) = \frac{1}{2^6} \left[ \frac{16R^2}{b^3} - \frac{4R^4}{b^5} + \frac{5R^5}{6b^6} \right], \quad 0 < R < 2b$$

$$W(R) = \frac{1}{2^6} \left[ -\frac{20R}{b^2} + \frac{56R^2}{b^3} - \frac{30R^3}{b^4} + \frac{6R^4}{b^5} - \frac{5R^5}{12b^6} \right], \quad 2b < R < 4b, \quad (II-46)$$

$$W(R) = \frac{1}{2^6} \left[ \frac{108R}{b^2} - \frac{72R^2}{b^3} + \frac{18R^3}{b^4} - \frac{2R^4}{b^5} + \frac{R^5}{12b^6} \right], \quad 4b < R < 6b.$$

The average values of  $\left\langle \frac{1}{R_{jk}} \right\rangle$  may be calculated from  $W_z(R)$  by multiplying the distribution function by  $\frac{1}{R}$  and integrating over all values of  $R$  from zero to infinity. That is,

$$\left\langle \frac{1}{R_{jk}} \right\rangle = \int_0^{\infty} \frac{1}{R} W_{|j-k|}(R) dR. \quad (II-47)$$

These have been computed for  $Z = |j-k|$  from 1 to 5.

$$Z = |j-k| = 1:$$

$$\left\langle \frac{1}{R_{jk}} \right\rangle = \frac{1}{b}, \quad (II-48)$$

$$Z = |j-k| = 2:$$

$$\left\langle \frac{1}{R_{jk}} \right\rangle = \frac{1}{b}, \quad (II-49)$$

$$Z = |j-k| = 3:$$

$$\left\langle \frac{1}{R_{jk}} \right\rangle = \frac{1}{4/3 b} = \frac{1}{1.333 b}, \quad (II-50)$$

$$Z = |j - k| = 4 :$$

$$\left\langle \frac{1}{R_{jk}} \right\rangle = \frac{1}{3/2 b} = \frac{1}{1.500 b} \quad (II-51)$$

$$Z = |j - k| = 5 :$$

$$\left\langle \frac{1}{R_{jk}} \right\rangle = \frac{1}{1.92/1.5 b} = \frac{1}{1.669 b} \quad (II-52)$$

When  $Z$  is very large (i.e.,  $|j - k| \gg 1$ ) the distribution function for  $W(\vec{R})$  is given by

$$W(\vec{R}) = \frac{1}{(2\pi Z b^2/3)^{3/2}} \cdot \exp\left(\frac{-3|\vec{R}|^2}{2 Z b^2}\right), \quad (II-53)$$

and the corresponding function for  $W(R)$  is

$$W(\vec{R}) = \frac{6R^2}{\left(\frac{2\pi}{3}\right)^{1/2} (Z b^2)^{3/2}} \cdot \exp\left(\frac{-3|\vec{R}|^2}{2 Z b^2}\right). \quad (II-54)$$

Results calculated using the distribution function given by equation (II-32) will be referred to as Treloar results.

If one takes an alternate view of the chain model as having a Gaussian distribution of segment length, then the distribution function for the displacement vector for a three dimensional random walk of  $Z = |j - k|$  steps, where the step length has a Gaussian distribution with a root mean square length of  $b$ , is given by Chandrasekhar (32) as

$$W_z(\vec{R}) = \frac{1}{(2\pi Z b^2/3)^{3/2}} \cdot \exp\left(\frac{-3R^2}{2 Z b^2}\right), \quad (II-55)$$

where  $b$  is now interpreted as the mean square length of each step.

This expression is exact for any value of  $Z$ . The distribution

function for  $|\vec{R}|$  is given by

$$W_z(R) = \frac{6 R^2}{\left(\frac{2\pi}{3}\right)^{1/2} (z b^2)^{3/2}} \exp\left(\frac{-3 R^2}{2 z b^2}\right). \quad (\text{II-56})$$

Note this is the same as the fixed step length distribution function for the case of  $z \gg 1$ . Equation (II-56) can be used to compute  $\langle \frac{1}{R_{jk}} \rangle$  for any value of  $z = |j-k|$  in the following way.

$$\begin{aligned} \left\langle \frac{1}{R_{jk}} \right\rangle &= \int_0^\infty \frac{1}{R} W_{|j-k|}(R) dR \\ &= \frac{6}{\left(\frac{2\pi}{3}\right)^{1/2} (z b^2)^{3/2}} \int_0^\infty R \exp\left(\frac{-3 R^2}{2 z b^2}\right) dR \\ &= \frac{6}{\left(\frac{2\pi}{3}\right)^{1/2} (z b^2)^{3/2}} \cdot \frac{1}{\left(\frac{3}{z b^2}\right)} \\ &= \left(\frac{6}{\pi}\right)^{1/2} \frac{1}{z^{1/2} b}. \end{aligned} \quad (\text{II-57})$$

Since  $z = |j-k|$ , this can be written as

$$\left\langle \frac{1}{R_{jk}} \right\rangle = \left(\frac{6}{\pi}\right)^{1/2} \frac{1}{|j-k|^{1/2} b}. \quad (\text{II-58})$$

This is the value used by Kirkwood and Riseman (7) for  $\langle \frac{1}{R_{jk}} \rangle$ , although they developed the expression by a different process. Values of  $\langle \frac{1}{R_{jk}} \rangle$  for  $|j-k| = 1$  to  $|j-k| = 5$  are given below.

$$|j-k| = 1: \quad \left\langle \frac{1}{R_{jk}} \right\rangle = \frac{1}{0.724 b}, \quad (\text{II-59})$$

$$|j-k| = 2: \quad \left\langle \frac{1}{R_{jk}} \right\rangle = \frac{1}{1.023 b}, \quad (\text{II-60})$$



$$|j-k|=3: \quad \left\langle \frac{1}{R_{jk}} \right\rangle = \frac{1}{1.253b} \quad (II-61)$$

$$|j-k|=4: \quad \left\langle \frac{1}{R_{jk}} \right\rangle = \frac{1}{1.448b} \quad (II-62)$$

$$|j-k|=5: \quad \left\langle \frac{1}{R_{jk}} \right\rangle = \frac{1}{1.616b} \quad (II-63)$$

Results calculated using equations (II-56) and (II-58) will be referred to as Kirkwood-Riseman values.

Using either the fixed or Gaussian distributed segment length model, the elements of the hydrodynamic interaction tensor are given by equation (II-30) as

$$\langle T_{jk} \rangle = \frac{1}{6\pi\eta_s} \left\langle \frac{1}{R_{jk}} \right\rangle. \quad (II-30)$$

From the nature of the application of  $\Pi$  given by equation (II-29),

$$\langle T_{jj} \rangle = 0, \quad 0 \leq j \leq N. \quad (II-64)$$

Then  $\Pi$  can be written as

$$\Pi = \frac{1}{6\pi\eta_s b} \begin{pmatrix} 0 & \left\langle \frac{b}{R_{12}} \right\rangle & \cdots & \left\langle \frac{b}{R_{1N}} \right\rangle \\ \left\langle \frac{b}{R_{21}} \right\rangle & 0 & \cdots & \\ \vdots & & \ddots & \\ \left\langle \frac{b}{R_{N1}} \right\rangle & \left\langle \frac{b}{R_{N2}} \right\rangle & \cdots & 0 \end{pmatrix}. \quad (II-65)$$

Thurston and Peterlin (17) have defined the segmental hydrodynamic interaction factor  $h^*$  as the approximate ratio of the hydrodynamic

radius of the bead to the segment length in the form

$$h^* = \frac{f}{(12\pi^3)^{1/2} \eta_s b} \quad , \quad (\text{II-66})$$

where  $f$  is the friction factor used in equation (II-10),  $\eta_s$  is the solvent viscosity, and  $b$  is the fixed or root mean square segment length, depending on the choice of the model version. Since

$$\frac{1}{6\pi\eta_s b} = \frac{h^*}{f} \cdot \left(\frac{\pi}{3}\right)^{1/2} \quad , \quad (\text{II-67})$$

$\Pi$  may be written as

$$\Pi = \frac{h^*}{f} \cdot \left(\frac{\pi}{3}\right)^{1/2} \cdot \begin{pmatrix} 0 & \langle \frac{b}{R_{12}} \rangle & \cdots & \langle \frac{b}{R_{1N}} \rangle \\ \langle \frac{b}{R_{21}} \rangle & 0 & \cdots & \langle \frac{b}{R_{2N}} \rangle \\ \vdots & \vdots & \ddots & \vdots \\ \langle \frac{b}{R_{N1}} \rangle & \langle \frac{b}{R_{N2}} \rangle & \cdots & 0 \end{pmatrix} \quad (\text{II-68})$$

or

$$\langle T_{jk} \rangle = \frac{h^*}{f} \cdot \left(\frac{\pi}{3}\right)^{1/2} \cdot b \cdot \left\langle \frac{1}{R_{jk}} \right\rangle \quad (\text{II-69})$$

The quantity  $h^*$  has zero for a lower limit, corresponding to the free draining condition of no hydrodynamic interaction. That  $h^*$  must have an upper bound is seen from the following simple argument. Consider one bead of the chain to be at the origin of a cartesian coordinate system and consider another bead of the model at the point  $(x_0, 0, 0)$ . Assume both beads to be immersed in a solvent initially at rest. Then by Burger's expression in equation (II-24), the perturbation in flow at the point  $(x_0, 0, 0)$  due to the motion of the bead at the origin will be

$$v_x = \frac{1}{8\pi\eta_s R} \left[ 1 + \frac{x_0^2}{R^2} \right] F_x^L \quad , \quad (\text{II-70})$$

where  $F_x^l$  is the  $x$ -component of the force exerted on the solvent by the motion of the bead at the origin. For simplicity, consider this bead to be moving in the  $+x$  direction. At the point  $(x_0, 0, 0)$ ,  $V_x$  becomes

$$V_x = \frac{F_x^l}{4\pi\eta_s R} . \quad (\text{II-71})$$

The force  $F_i$  exerted on the bead at  $(x_0, 0, 0)$  by the perturbation velocity of the solvent is given in the form of equation (II-10) as

$$\begin{aligned} F_i &= -f V_x \\ &= \frac{-f F_x^l}{4\pi\eta_s R} . \end{aligned} \quad (\text{II-72})$$

Since  $|F_i|$  cannot exceed  $|F_x^l|$ , or

$$\left| \frac{F_i}{F_x^l} \right| \leq 1, \quad (\text{II-73})$$

it follows that

$$\frac{f}{4\pi\eta_s R} \leq 1 . \quad (\text{II-74})$$

Consider the particular case where the beads are nearest neighbors on the chain. Taking the Treloar value for  $\left\langle \frac{1}{R} \right\rangle$  for nearest neighbors, equation (II-73) becomes

$$\frac{f}{4\pi\eta_s b} \leq 1 . \quad (\text{II-75})$$

Using the results of equation (II-66), this becomes

$$\left( \frac{3\pi}{4} \right)^{1/2} h^* \leq 1 \quad (\text{II-76})$$

or

$$h^* \leq \left( \frac{4}{3\pi} \right)^{1/2} . \quad (\text{II-77})$$

Thus

$$h^* \leq 0.652 \quad (\text{II-78})$$

for this simple case of nearest neighbors and one dimensional motion. Although the limits on  $h^*$  by this means of analysis depend upon the distance  $\langle \frac{1}{R_{jk}} \rangle$  and thus upon the particular choice of beads taken for analysis, the point is still valid that  $h^*$  cannot take on large values.

Note that  $\Pi$  is a symmetric matrix, since  $\langle \frac{1}{R_{jk}} \rangle$  is only a function of  $|j-k|$ , by equation (II-47) or (II-57).

#### The Diffusion Equation and Normal Coordinates

Returning to the equation of motion of the chain,  $\vec{\chi}$  is given by equation (II-16) as

$$\begin{aligned} \vec{\chi} = \vec{\chi}_\ell + f' \left[ -\frac{3kT}{b^2} \mathbb{A} \cdot \vec{\chi} \right. \\ \left. - \mathcal{H}(\vec{\chi} - \vec{\chi}_\Omega) - kT \vec{\nabla}_\chi \ln \Psi \right]. \end{aligned} \quad (\text{II-16})$$

And, by equation (II-17),

$$\vec{\dot{\chi}}_\ell = \vec{\dot{\chi}}_\ell^0 - \Pi \cdot \vec{F}_\chi \quad (\text{II-17})$$

Substituting the value of  $\vec{F}_\chi$  given by equation (II-11) yields

$$\vec{\dot{\chi}}_\ell = \vec{\dot{\chi}}_\ell^0 + \Pi \left[ f(\vec{\chi} - \vec{\chi}_\ell) \right]. \quad (\text{II-79})$$

Substituting the value of  $f(\vec{\chi} - \vec{\chi}_\ell)$  given by equation (II-15) yields

$$\begin{aligned} \vec{\dot{\chi}} = \vec{\dot{\chi}}_\ell + \Pi \cdot \left[ -\frac{3kT}{b^2} \mathbb{A} \cdot \vec{\chi} \right. \\ \left. - \mathcal{H}(\vec{\chi} - \vec{\chi}_\Omega) - kT \vec{\nabla}_\chi \ln \Psi \right]. \end{aligned} \quad (\text{II-80})$$

Substituting this into equation (II-16) gives

$$\begin{aligned} \vec{X} = \vec{X}_\ell^0 + \pi \cdot \left[ -\frac{3kT}{b^2} \mathbf{A} \cdot \vec{x} - \mathcal{F}(\vec{x} - \vec{x}_\Omega) - kT \vec{\nabla}_x \ln \psi \right] \\ + f^{-1} \left[ -\frac{3kT}{b^2} \mathbf{A} \cdot \vec{x} - \mathcal{F}(\vec{x} - \vec{x}_\Omega) - kT \vec{\nabla}_x \ln \psi \right], \end{aligned}$$

or

$$\begin{aligned} \vec{X} = \vec{X}_\ell^0 + f^{-1} (f\pi + \mathbb{1}) \cdot \left[ -\frac{3kT}{b^2} \mathbf{A} \cdot \vec{x} \right. \\ \left. - \mathcal{F}(\vec{x} - \vec{x}_\Omega) - kT \vec{\nabla}_x \ln \psi \right], \quad (\text{II-81}) \end{aligned}$$

where  $\mathbb{1}$  is the identity  $(N+1) \times (N+1)$  matrix. Now, let

$$\mathbb{H} = f\pi + \mathbb{1}. \quad (\text{II-82})$$

Then, using equation (II-68), the space average values of the elements of  $\mathbb{H}$  are given by

$$H_{jk} = h^* \left( \frac{\pi}{3} \right)^{1/2} b \left\langle \frac{1}{R_{jk}} \right\rangle, \quad j \neq k, \quad (\text{II-83})$$

$$H_{jj} = 1.$$

Since  $\left\langle \frac{1}{R_{jk}} \right\rangle$  is a real multiple of  $b$ , then the elements of  $\mathbb{H}$  are dimensionless and real.

Carrying out the multiplication equation in (II-71) yields

$$\begin{aligned} \vec{X} = \vec{X}_\ell^0 - \left[ f^{-1} \frac{3kT}{b^2} \mathbb{H} \cdot \mathbf{A} \cdot \vec{x} \right. \\ \left. + f^{-1} \mathbb{H} \cdot \mathcal{F}(\vec{x} - \vec{x}_\Omega) + f^{-1} kT \mathbb{H} \vec{\nabla}_x \ln \psi \right]. \quad (\text{II-84}) \end{aligned}$$

Now still following the formalism of Cerf (13), let

$$D = \frac{kT}{f}, \quad (\text{II-85})$$

and let

$$\delta = \frac{3kT}{fb^2}. \quad (\text{II-86})$$

Then equation (II-84) becomes

$$\begin{aligned} \dot{\vec{x}} = \dot{\vec{x}}_e - \left[ \delta H \cdot A \cdot \vec{x} + f^{-1} H \cdot \mathcal{H} \cdot (\vec{x} - \vec{x}_e) \right. \\ \left. + D H \vec{\nabla}_x \ln \psi \right]. \end{aligned} \quad (\text{II-87})$$

The distribution function  $\psi$  must satisfy an equation of continuity given by

$$\frac{\partial \psi}{\partial t} = -\text{div } \psi (\vec{x} + \vec{y} + \vec{z}). \quad (\text{II-88})$$

Using equation (II-87) for  $\vec{x}$  and similar expressions for  $\vec{y}$  and  $\vec{z}$  yields

$$\begin{aligned} \frac{\partial \psi}{\partial t} = \sum_{x,y,z} \vec{\nabla}_x^T \psi \left[ -\dot{\vec{x}}_e + D H \vec{\nabla}_x \ln \psi \right. \\ \left. + \delta H \cdot A \cdot \vec{x} + f^{-1} H \cdot \mathcal{H} (\vec{x} - \vec{x}_e) \right], \end{aligned} \quad (\text{II-89})$$

where the form  $\vec{\nabla}_x^T$  is used because the bracketed quantity is a column vector. The sum indicates the inclusion of analogous quantities in  $y$  and  $z$ .

Since the matrices in equation (II-89) are not in general diagonal, the matrices are diagonalized by transforming to a set of normal coordinates according to

$$\begin{aligned} \vec{u} &= Q^{-1} \vec{x} \\ \vec{v} &= Q^{-1} \vec{y} \\ \vec{w} &= Q^{-1} \vec{z}, \end{aligned} \quad (\text{II-90})$$

where  $\vec{u}$ ,  $\vec{v}$ , and  $\vec{w}$  are the normal coordinates and the columns of  $\mathbb{Q}$  are the eigenvectors of the product  $\mathbb{H} \cdot \mathbb{A}$  (34). The eigenvalue equation from which the eigenvectors  $\vec{\alpha}_p$  and eigenvalues  $\lambda_p$  of  $\mathbb{H} \cdot \mathbb{A}$  are obtained is

$$\mathbb{H} \cdot \mathbb{A} \cdot \vec{\alpha}_p = \lambda_p \vec{\alpha}_p. \quad (\text{II-91})$$

The components of  $\vec{\alpha}_p$  are used to form the  $p$ -th column of  $\mathbb{Q}$  and therefore by equation (II-91)

$$\mathbb{Q}^{-1} \cdot \mathbb{H} \cdot \mathbb{A} \cdot \mathbb{Q} = \mathbb{\Lambda}, \quad (\text{II-92})$$

where  $\mathbb{\Lambda}$  is the diagonal matrix whose diagonal elements are the eigenvalues  $\lambda_p$  of the matrix  $\mathbb{H} \cdot \mathbb{A}$ .  $\mathbb{H}$  has been observed to be symmetric and  $\mathbb{A}$  is symmetric by equation (II-6). Thus

$$\begin{aligned} \mathbb{H} &= \mathbb{H}^T, \\ \mathbb{A} &= \mathbb{A}^T. \end{aligned} \quad (\text{II-93})$$

Using these facts and the algebraic properties of matrices (34), the following observations can be made.

$$\begin{aligned} \vec{\alpha}_p^T \mathbb{A} \cdot \mathbb{H} &= (\mathbb{H}^T \cdot \mathbb{A}^T \cdot \vec{\alpha}_p)^T = (\mathbb{H} \cdot \mathbb{A} \cdot \vec{\alpha}_p)^T \\ &= (\lambda_p \vec{\alpha}_p)^T, \end{aligned}$$

or

$$\vec{\alpha}_p^T \mathbb{A} \cdot \mathbb{H} = \lambda_p \vec{\alpha}_p^T. \quad (\text{II-94})$$

Then

$$\begin{aligned} \vec{\alpha}_p^T \mathbb{A} \cdot \mathbb{H} \cdot \mathbb{A} \cdot \vec{\alpha}_2 &= (\vec{\alpha}_p^T \cdot \mathbb{A} \cdot \mathbb{H}) \cdot \mathbb{A} \cdot \vec{\alpha}_2 \\ &= \lambda_p \vec{\alpha}_p^T \mathbb{A} \cdot \vec{\alpha}_2. \end{aligned} \quad (\text{II-95})$$

But by distributing the above multiplication another way,

$$\begin{aligned}
 \vec{\alpha}_p^T A \cdot H \cdot A \cdot \vec{\alpha}_l &= \vec{\alpha}_p^T A (H \cdot A) \vec{\alpha}_l \\
 &= \vec{\alpha}_p^T A \lambda_l \vec{\alpha}_l \\
 &= \lambda_l \vec{\alpha}_p^T A \cdot \vec{\alpha}_l.
 \end{aligned} \tag{II-96}$$

Thus

$$\lambda_p (\vec{\alpha}_p^T A \vec{\alpha}_l) = \lambda_l (\vec{\alpha}_p^T A \vec{\alpha}_l). \tag{II-97}$$

These can be identically equal only if  $\vec{\alpha}_p^T A \vec{\alpha}_l = 0$  for  $p \neq l$ .

For  $p=l$  the equality follows immediately. Therefore, if all the eigenvalues are distinct,  $A$  is diagonalized by the congruent transformation

$$Q^T A Q = M, \tag{II-98}$$

where  $M$  has nonzero elements  $\mu_k$  on the diagonal only.

Equation (II-98) provides a method to calculate  $Q^{-1}$ . Multiplying on the left with  $M^{-1}$  yields

$$M^{-1} Q^T A Q = M^{-1} M = \mathbb{1}.$$

Right multiplying this by  $Q^{-1}$  yields

$$M^{-1} Q^T A Q Q^{-1} = \mathbb{1} \cdot Q^{-1}$$

or

$$M^{-1} Q^T A = Q^{-1} \tag{II-99}$$

This allows the construction of  $Q^{-1}$  without the necessity of algebraically inverting  $Q$ . Since  $\mu_0$  turns out to be zero, the first row



of  $Q^{-1}$  is indeterminate by this method. Now define a set of  $N+1$  vectors  $\vec{\beta}_p$  as the column vectors of  $Q^{-1T}$ . From equation (II-92)

$$(Q^{-1} H A Q)^T = (\Lambda)^T,$$

$$Q^T A^T H^T Q^{-1T} = \Lambda^T = \Lambda,$$

or

$$Q^T A H Q^{-1T} = \Lambda. \quad (\text{II-100})$$

Thus the vectors  $\vec{\beta}_p$  are the eigenvectors of  $A H$  with eigenvalues still given by  $\lambda_p$ . By equation (II-98),

$$A Q = Q^{-1T} M \quad (\text{II-101})$$

Substituting this value into equation (II-92) yields

$$Q^{-1} H Q^{-1T} M = \Lambda,$$

or

$$Q^{-1} H Q^{-1T} = \Lambda M^{-1} = N. \quad (\text{II-102})$$

Thus  $N$  is diagonal with elements  $\nu_p$  given by

$$\nu_p = \vec{\beta}_p^T H \vec{\beta}_p, \quad (\text{II-103})$$

or, since  $\Lambda M^{-1} = N$ ,

$$\nu_p = \frac{\lambda_p}{\mu_p}. \quad (\text{II-104})$$

Again,  $\nu_0$  is indeterminate in this expression, since  $\lambda_0$  and  $\mu_0$  turn out to be zero.  $\nu_0$  is determined from equation (II-103), but this

requires the inversion of  $\mathbb{Q}$  to find the  $\vec{\beta}_p$  values.

Cerf uses the matrix  $\mathbb{Q}$  to define the matrix  $\mathbb{H}$  which was only stated earlier in equation (II-7) without explanation. Cerf uses the form

$$\mathbb{H} = \mathbb{Q}^{-T} \mathbb{\Phi} \mathbb{Q}^{-1}, \quad (\text{II-105})$$

where  $\mathbb{\Phi}$  is the diagonal matrix of internal viscosity. Now, making the substitution

$$\mathbb{R} = f^{-1} \mathbb{\Phi}, \quad (\text{II-106})$$

with diagonal elements  $\rho_p$  only, equation (II-87) can be written as

$$\begin{aligned} \vec{\dot{x}} = \vec{\dot{x}}_0 - \left[ \delta \mathbb{H} \cdot \mathbb{A} \cdot \vec{x} + \mathbb{H} \mathbb{Q}^{-T} \mathbb{R} \mathbb{Q}^{-1} (\vec{x} - \vec{x}_\infty) \right. \\ \left. + \mathbb{H} \cdot \mathbb{D} \vec{\nabla}_x \ln \psi \right]. \end{aligned} \quad (\text{II-107})$$

This can now be put in normal coordinate form by multiplying on the left by  $\mathbb{Q}^{-1}$  and using the transformation relations of equation (II-90). Then

$$\begin{aligned} \mathbb{Q}^{-1} \vec{\dot{x}} &= \mathbb{Q}^{-1} \vec{\dot{x}}_0 - \delta \mathbb{Q}^{-1} \mathbb{H} \mathbb{A} \vec{x} - \mathbb{Q}^{-1} \mathbb{H} \mathbb{Q}^{-T} \mathbb{R} \mathbb{Q}^{-1} (\vec{x} - \vec{x}_\infty) \\ &\quad - \mathbb{Q}^{-1} \mathbb{H} \mathbb{D} \vec{\nabla}_x \ln \psi \\ &= \vec{\dot{u}}_0 - \delta \mathbb{Q}^{-1} \mathbb{H} \mathbb{A} \mathbb{Q} \mathbb{Q}^{-1} \vec{x} - \mathbb{N} \cdot \mathbb{R} (\vec{u} - \vec{u}_\infty) \\ &\quad - \mathbb{Q}^{-1} \mathbb{H} \mathbb{Q}^{-T} \mathbb{Q}^T \mathbb{D} \vec{\nabla}_x \ln \psi \\ &= \vec{\dot{u}}_0 - \delta \mathbb{N} \vec{u} - \mathbb{N} \mathbb{R} (\vec{u} - \vec{u}_\infty) - \mathbb{N} \mathbb{D} \mathbb{Q}^{-T} \vec{\nabla}_x \ln \psi. \end{aligned} \quad (\text{II-108})$$

Since the partial derivatives transform according to

$$\begin{aligned} \partial / \partial \vec{x} &= \mathbb{Q}^{-T} \partial / \partial \vec{u} \\ \partial / \partial \vec{u} &= \mathbb{Q}^T \partial / \partial \vec{x}, \end{aligned} \quad (\text{II-109})$$

equation (II-108) may be written as

$$\begin{aligned}\vec{u} &= \vec{u}_d^0 - \delta N \cdot M \vec{u} - N R (\vec{u} - \vec{u}_\infty) \\ &\quad - D N \vec{\nabla}_u \ln \psi.\end{aligned}\quad (\text{II-110})$$

Solving for

$$\vec{u}_d = (\vec{u} - \vec{u}_\infty), \quad (\text{II-111})$$

which is the rate of deformation of the normal coordinates, yields

$$\begin{aligned}R^{-1} N^{-1} \vec{u} &= R^{-1} N^{-1} \vec{u}_d^0 - \delta R^{-1} M \vec{u} \\ &\quad - (\vec{u} - \vec{u}_\infty) - D R^{-1} \vec{\nabla}_u \ln \psi,\end{aligned}$$

or

$$\begin{aligned}(\vec{u} - \vec{u}_\infty) &= R^{-1} N^{-1} (\vec{u}_d^0 - \vec{u}) - \delta R^{-1} M \vec{u} \\ &\quad - D R^{-1} \vec{\nabla}_u \ln \psi.\end{aligned}\quad (\text{II-112})$$

In terms of the  $\rho$ -th component of  $\vec{u}_d$ , this can be written as

$$\dot{u}_{d,\rho} = \frac{1}{\rho_\rho v_\rho} (\dot{u}_{d,\rho}^0 - \dot{u}_\rho) - \frac{\delta}{\rho_\rho} \mu_\rho u_\rho - \frac{D}{\rho_\rho} \frac{\partial}{\partial u_\rho} \ln \psi,$$

or

$$\begin{aligned}\dot{u}_{d,\rho} &= \frac{1}{\rho_\rho v_\rho} \left[ \dot{u}_{d,\rho}^0 - \dot{u}_\rho - \delta v_\rho \mu_\rho u_\rho \right. \\ &\quad \left. - D v_\rho \frac{\partial}{\partial u_\rho} \ln \psi \right].\end{aligned}\quad (\text{II-113})$$

But by equation (II-111),

$$\dot{u}_\rho = \dot{u}_{d,\rho} + \dot{u}_{\infty,\rho}. \quad (\text{II-114})$$

Thus

$$\dot{u}_{d,p} = \frac{1}{\rho_p v_p} \left[ \dot{u}_{l,p}^{\circ} - \dot{u}_{\Omega,p} - \dot{u}_{d,p} - v_p \left( \delta \mu_p u_p + D \frac{\partial}{\partial u_p} \ln \psi \right) \right],$$

or

$$\dot{u}_{d,p} \left( 1 + \frac{1}{\rho_p v_p} \right) = \left[ \dot{u}_{l,p}^{\circ} - \dot{u}_{\Omega,p} - v_p \left( \delta \mu_p u_p + D \frac{\partial}{\partial u_p} \ln \psi \right) \right]. \quad (\text{II-115})$$

Thus

$$\dot{u}_{d,p} = \frac{-1}{\rho_p v_p + 1} \left[ -\dot{u}_{l,p}^{\circ} + \dot{u}_{\Omega,p} + v_p \left( \delta \mu_p u_p + D \frac{\partial}{\partial u_p} \ln \psi \right) \right]. \quad (\text{II-116})$$

Since the applied motion is  $\vec{\dot{x}}_l^{\circ} = G \vec{z}$ , this can be transformed to normal coordinate form by

$$Q^{-1} \vec{\dot{x}}_l^{\circ} = Q^{-1} G \vec{z},$$

or

$$\vec{\dot{u}}_l^{\circ} = G \vec{w}. \quad (\text{II-117})$$

Thus, in equation (II-116),

$$\dot{u}_{l,p}^{\circ} = G w_p \quad (\text{II-118})$$

Similarly,

$$\dot{v}_{l,p}^{\circ} = \dot{w}_{l,p}^{\circ} = 0, \quad (\text{II-119})$$

from equation (II-23). Therefore, for  $\vec{W}$  (or  $\vec{V}$ ), equation (II-116) can be written as

$$\dot{w}_{d,p} = \frac{-1}{\rho_p \psi_p + 1} \left[ \psi_p (\delta \mu_p w_p + D \frac{\partial}{\partial w_p} \ln \psi) + \dot{w}_{\Omega,p} \right]. \quad (\text{II-120})$$

The continuity equation, equation (II-89), can be put in normal coordinate form by application of equation (II-109) to form

$$\begin{aligned} \vec{\nabla}_x &= Q^{-1T} \vec{\nabla}_u, \\ \vec{\nabla}_u &= Q^T \vec{\nabla}_x, \end{aligned} \quad (\text{II-121})$$

and, taking the transpose of each side,

$$\begin{aligned} \vec{\nabla}_x^T &= (Q^{-1T} \vec{\nabla}_u)^T \\ &= \vec{\nabla}_u^T (Q^{-1T})^T, \end{aligned}$$

or

$$\vec{\nabla}_x^T = \vec{\nabla}_u^T Q^{-1}. \quad (\text{II-122})$$

Substitution of this value into equation (II-89) yields

$$\begin{aligned} \frac{\partial \psi}{\partial t} &= \sum_x \vec{\nabla}_u^T Q^{-1} \left[ \psi (-\vec{x}_\ell^0 + \delta H \cdot A \vec{x} \right. \\ &\quad \left. + H \cdot Q^{-1T} R Q^{-1} (\vec{x} - \vec{x}_\Omega)) + \psi D H \vec{\nabla}_x \ln \psi \right]. \end{aligned} \quad (\text{II-123})$$

Since

$$\vec{\nabla}_x \ln \psi = \frac{1}{\psi} \vec{\nabla}_x \psi, \quad (\text{II-124})$$

equation (II-123) can be written as

$$\begin{aligned} \frac{\partial \psi}{\partial t} = \sum_x \vec{\nabla}_u^T & \left[ \psi \left( -Q^{-1} \vec{x}_x^0 + \delta Q^{-1} H \cdot A Q Q^{-1} \vec{x} \right. \right. \\ & \left. \left. + Q^{-1} H \cdot Q^{-T} R Q^{-1} (\vec{x} - \vec{x}_\Omega) \right) \right. \\ & \left. + D Q^{-1} H Q^{-T} Q^T \vec{\nabla}_x \psi \right]. \end{aligned}$$

Or,

$$\begin{aligned} \frac{\partial \psi}{\partial t} = \sum_{u,v,w} \vec{\nabla}_u^T & \left[ \psi \left( -\vec{u}_x^0 + \delta N \cdot M \vec{u} \right. \right. \\ & \left. \left. + N R (\vec{u} - \vec{u}_\Omega) \right) + D N \vec{\nabla}_u \psi \right], \end{aligned} \quad (\text{II-125})$$

since  $Q^T \vec{\nabla}_x = \vec{\nabla}_u$  by equation (II-121). Since by definition

$$\vec{\nabla}_u^T = \sum_{p=0}^N \frac{\partial}{\partial u_p}, \quad (\text{II-126})$$

equation (II-125) may be written in terms of the matrix components in the following way.

$$\begin{aligned} \frac{\partial \psi}{\partial t} = \sum_{u,v,w} \left\{ \sum_{p=0}^N \frac{\partial}{\partial u_p} \left[ \psi \left( -\dot{u}_{x,p}^0 + \delta v_p \mu_p u_p \right. \right. \right. \\ \left. \left. \left. + v_p \rho_p (\dot{u}_{x,p}) \right) + D v_p \frac{\partial \psi}{\partial u_p} \right] \right\}. \end{aligned} \quad (\text{II-127})$$

Substituting the value of  $\dot{u}_{x,p}$  given by equation (II-116) into equation (II-127) yields

$$\begin{aligned} \frac{\partial \psi}{\partial t} = \sum_{p=0}^N \sum_{u,v,w} \frac{\partial}{\partial u_p} & \left[ \frac{-1}{1+v_p \rho_p} \right] \left[ \dot{u}_{x,p}^0 \psi \right. \\ & \left. - \delta \lambda_p u_p \psi - D v_p \frac{\partial \psi}{\partial u_p} + \dot{u}_{\Omega,p} v_p \rho_p \psi \right], \end{aligned} \quad (\text{II-128})$$

where the order of summation has been interchanged. This can be simplified by making the following observations. By equations (II-118) and (II-119),

$$\begin{aligned}\dot{u}_{l,p}^0 &= G w_p, \\ \dot{v}_{l,p}^0 &= 0, \\ \dot{w}_{l,p}^0 &= 0.\end{aligned}$$

By the geometry of the problem,

$$\vec{\dot{y}}_{\Omega} = 0, \quad (\text{II-129})$$

so

$$\vec{\dot{V}}_{\Omega} = Q^{-1}(\vec{\dot{y}}_{\Omega}) = 0. \quad (\text{II-130})$$

Therefore the terms  $-\delta\lambda_p u_p$  and  $-Dv_p \frac{\partial \psi}{\partial u_p}$  exist for  $u$ ,  $v$ , and  $w$ . The term  $\dot{u}_{l,p}^0 \psi$  exists only for  $u$ , and the term  $v_p \rho_p \dot{u}_{l,p}^0 \psi$  exists only for  $u$  and  $w$ . Thus equation (II-125) may be written in the form given by Cerf as

$$\begin{aligned}\frac{\partial \psi}{\partial t} = & - \sum_{p=0}^N \left( \frac{1}{v_p \rho_p + 1} \right) \left[ G w_p \frac{\partial \psi}{\partial u_p} + \rho_p v_p \left( \frac{\partial}{\partial u_p} (\psi \dot{u}_{l,p}^0) \right) \right. \\ & \left. + \frac{\partial}{\partial w_p} (\psi \dot{w}_{l,p}^0) \right] - \sum_{u,v,w} \left( D v_p \frac{\partial^2 \psi}{\partial u_p^2} + \delta \lambda_p (\psi + u_p \frac{\partial \psi}{\partial u_p}) \right) \Big]. \quad (\text{II-131})\end{aligned}$$

This is the diffusion equation in normal coordinate form. By placing the origin of the coordinate system at the center of resistance of the chain,  $u_0 = v_0 = w_0 = 0$  and the summation can be taken from  $p=1$  to  $p=N$ . The equation need not be solved completely, since

the average values that are necessary to calculate the intrinsic viscosity of the solvent-polymer solution may be obtained from a form of equation (II-131). Considering the steady state form of equation (II-131) (i.e.,  $\frac{\partial \psi}{\partial t} = 0$ ), Cerf uses the method of separation of variables and considers the distribution function of  $u_p$  and  $w_p$  denoted by  $\phi(u_p w_p)$  and defined by

$$\psi(u_p, v_p, w_p) = \phi(u_p, w_p) \exp\left(-\frac{\delta}{2D}\right) \sum_{p=1}^N \mu_p v_p^2 \quad (\text{II-132})$$

The function  $\phi$  must then satisfy the equation

$$0 = \sum_{p=1}^N \frac{1}{1 + \rho_p v_p} \left[ G w_p \frac{\partial \phi}{\partial u_p} + \rho_p v_p \left( \frac{\partial}{\partial u_p} (\phi \dot{u}_{1p}) + \frac{\partial}{\partial w_p} (\phi \dot{w}_{1p}) \right) \right. \quad (\text{II-133})$$

$$\left. - D v_p \left( \frac{\partial^2 \phi}{\partial u_p^2} + \frac{\partial^2 \phi}{\partial w_p^2} \right) - \delta \lambda_p \left( \frac{\partial}{\partial u_p} (u_p \phi) + \frac{\partial}{\partial w_p} (w_p \phi) \right) \right].$$

By multiplying equation (II-133) successively by  $u_p^2$ ,  $w_p^2$ ,  $u_p w_p$ , and integrating over the entire configuration space, the following relations are obtained:

$$G \langle u_p w_p \rangle + \rho_p v_p \langle -\Omega u_p w_p \rangle + D v_p - \delta \lambda_p \langle u_p^2 \rangle = 0, \quad (\text{II-134})$$

$$-\rho_p v_p \langle -\Omega u_p w_p \rangle + D v_p - \delta \lambda_p \langle w_p^2 \rangle = 0, \quad (\text{II-135})$$

$$G \langle w_p^2 \rangle - \rho_p v_p \langle -\Omega (u_p^2 - w_p^2) \rangle - 2 \delta \lambda_p \langle u_p w_p \rangle = 0. \quad (\text{II-136})$$



where the symbol  $\langle \dots \rangle$  indicates the space average of the value enclosed over the configuration space. For example

$$\langle u_p^2 \rangle = \int u_p^2 \phi du_1 \dots dw_N, \quad (\text{II-137})$$

where the average could equally well be over the function  $\psi$ .  $\Omega$  is the instantaneous velocity of rotation of the molecule about the  $y$  axis and thus defines  $\vec{x}_\Omega$  and  $\vec{z}_\Omega$  as

$$\begin{aligned} \vec{x}_\Omega &= \Omega \vec{z}, \\ \vec{z}_\Omega &= -\Omega \vec{x}. \end{aligned} \quad (\text{II-138})$$

Applying the normal coordinate transformation to these equations yields

$$\begin{aligned} \vec{u}_\Omega &= Q^{-1} \vec{x}_\Omega = \Omega Q^{-1} \vec{z} = \Omega \vec{w}, \\ \vec{w}_\Omega &= Q^{-1} \vec{z}_\Omega = -\Omega Q^{-1} \vec{x} = -\Omega \vec{u}, \end{aligned}$$

or

$$\begin{aligned} \vec{u}_\Omega &= \Omega \vec{w} \\ \vec{w}_\Omega &= -\Omega \vec{u}. \end{aligned} \quad (\text{II-139})$$

Equation (II-134) will be derived to illustrate the method followed in obtaining such averages. Several preliminary results will first be calculated using  $\eta_k$  as a dummy variable. The assumption must be made that both  $\psi$  and  $\phi$  go to zero as any of the arguments goes to infinity more rapidly than any power of the argument. The first integral needed is

$$\begin{aligned} \int_{-\infty}^{\infty} \eta_k \frac{\partial \phi}{\partial \eta_k} d\vec{u}^N &= \left[ \eta_k \phi \right]_{-\infty}^{\infty} - \int \phi d\vec{u}^N \\ &= 0 - J^{-1} = -J^{-1}, \end{aligned} \quad (\text{II-140})$$

where  $J$  is the Jacobian of the coordinate system defined by

$$\int \phi du, \dots dw_N = J^{-1}, \quad (\text{II-141})$$

and

$$d\vec{u}^N = du, \dots dw_N. \quad (\text{II-142})$$

Also,

$$\begin{aligned} \int \eta_k^2 \frac{\partial^2 \phi}{\partial \eta_k^2} d\vec{u}^N &= \left[ \eta_k^2 \phi \right]_{-\infty}^{\infty} - \int 2\eta_k \left( \frac{\partial \phi}{\partial \eta_k} \right) d\vec{u}^N \\ &= 0 - 2(-J^{-1}), \end{aligned} \quad (\text{II-143})$$

by equation (II-140). Thus

$$\int \eta_k^2 \frac{\partial^2 \phi}{\partial \eta_k^2} d\vec{u}^N = 2J^{-1} \quad (\text{II-144})$$

Finally,

$$\begin{aligned} \int f(w_p, v_p) u_p^2 \frac{\partial \phi}{\partial u_p} d\vec{u}^N \\ &= \left[ f(w_p, v_p) u_p^2 \phi \right]_{-\infty}^{\infty} - \int 2f(w_p, v_p) u_p \phi d\vec{u}^N \\ &= -2 \langle f(w_p, v_p) u_p \rangle. \end{aligned} \quad (\text{II-145})$$

Since the averages to be formed from II-123 are formed by integrating over the position coordinates, the relation

$$\int f(\phi, u_p, v_p, w_p) d\vec{r}^N = J \int f(\phi, u_p, v_p, w_p) d\vec{u}^N \quad (\text{II-146})$$

will be used to change the form of equations (II-141), (II-144), and (II-145).  $d\vec{r}^N$  is the volume element in position coordinate space.

The equations then take the form

$$\int n_k \frac{\partial \Phi}{\partial n_k} d\vec{r}^N = -1 ,$$

$$\int n_k^2 \frac{\partial^2 \Phi}{\partial n_k^2} d\vec{r}^N = 2 , \quad (\text{II-147})$$

$$\int f(\omega_p, \nu_p) u_p^2 \frac{\partial \Phi}{\partial u_p} d\vec{r}^N = -2 \langle f(\omega_p, \nu_p) u_p \rangle J.$$

Multiplying equation (II-133) by  $u_p^2$  and integrating over all space leaves only those terms of the summation with the index  $p$ , since  $u_p$  and  $u_k$  are linearly independent. Thus equation (II-123) becomes

$$\frac{1}{1+\rho_p \nu_p} \left[ \int_{-\infty}^{\infty} G \omega_p u_p^2 \frac{\partial \Phi}{\partial u_p} d\vec{r}^N + \rho_p \nu_p \int u_p^2 \frac{\partial}{\partial u_p} (\phi \dot{u}_{2,p}) d\vec{r}^N \right. \\ \left. + \rho_p \nu_p \int u_p^2 \frac{\partial}{\partial \omega_p} (\phi \dot{u}_{2,p}) d\vec{r}^N - D \nu_p \int u_p^2 \frac{\partial^2 \Phi}{\partial u_p^2} d\vec{r}^N \right. \\ \left. - D \nu_p \int u_p^2 \frac{\partial^2 \Phi}{\partial \omega_p^2} d\vec{r}^N - \delta \lambda_p \int u_p^2 \frac{\partial}{\partial u_p} (u_p \Phi) d\vec{r}^N \right. \\ \left. - \delta \lambda_p \int u_p^2 \frac{\partial}{\partial \omega_p} (\omega_p \Phi) d\vec{r}^N \right] = 0. \quad (\text{II-148})$$

Using equation (II-138) and the fact that  $u_p, \omega_p$  and  $\nu_p$  are orthogonal allows equation (II-148) to be written as

$$G \int \omega_p u_p^2 \frac{\partial \Phi}{\partial u_p} d\vec{r}^N + \rho_p \nu_p \int u_p^2 \Omega \omega_p \frac{\partial \Phi}{\partial u_p} d\vec{r}^N \\ - D \nu_p \int u_p^2 \frac{\partial^2 \Phi}{\partial u_p^2} d\vec{r}^N - \delta \lambda_p \int u_p^2 [u_p \frac{\partial \Phi}{\partial u_p} + \Phi] d\vec{r}^N \\ = 0. \quad (\text{II-149})$$

Or, using equations (II-147),

$$\begin{aligned} & -2G \langle w_p u_p \rangle J - \rho_p v_p 2 \langle \Omega u_p w_p \rangle J \\ & - 2Dv_p - \delta\lambda_p [-3 \langle u_p^2 \rangle J + \langle u_p^4 \rangle J] = 0, \end{aligned} \quad (\text{II-150})$$

or

$$\begin{aligned} & G \langle u_p^2 w_p \rangle J + \rho_p v_p \langle \Omega u_p w_p \rangle J + Dv_p \\ & + \delta\lambda_p \langle u_p^2 \rangle J = 0. \end{aligned} \quad (\text{II-151})$$

Following Cerf and taking the Jacobian of the system as one, equation (II-134) follows immediately. Equations (II-135) and (II-136) are derived in the same way. These three equations constitute three equations in three unknowns:  $\langle u_p^2 \rangle$ ,  $\langle w_p^2 \rangle$ ,  $\langle u_p w_p \rangle$ . Solving for  $\langle u_p w_p \rangle$  yields

$$\langle u_p w_p \rangle = \frac{D G v_p}{2(\delta\lambda_p)^2 + \frac{\rho_p v_p G^2}{2}(2 + \rho_p v_p)} \quad (\text{II-152})$$

which can be written in the form given by Cerf as

$$\langle u_p w_p \rangle = \frac{D \tau_p G}{\delta\mu_p} \cdot \frac{1}{1 + \rho_p v_p (2 + \rho_p v_p) \tau_p^2 G^2}, \quad (\text{II-153})$$

where  $\tau_p$  is given by

$$\tau_p = \frac{1}{2\delta\lambda_p} \quad (\text{II-154})$$

#### The Application of the Eigenvalues to the Intrinsic Viscosity

Burger's treatment of the intrinsic viscosity of particles in solution yields the following expression:

$$[\eta] = \frac{N_a}{M\eta_s G} \left\langle \sum_{i=0}^N z_i F_{x,i} \right\rangle, \quad (\text{II-155})$$

where  $N_a$  is Avogadro's number,  $M$  is the molecular weight,  $z_i$  is the  $z$ -coordinate of the  $i$ -th bead of the chain and  $F_{x,i}$  is the  $x$ -component of the force exerted on the  $i$ -th bead by the solvent (13).

In the case of small internal viscosity, the rate of rotation of the molecule can be given by

$$\Omega = \frac{G}{2}. \quad (\text{II-156})$$

In this special case Cerf has shown the average in equation (II-155) to be

$$\left\langle \sum_{i=0}^N z_i F_{x,i} \right\rangle = f \delta \sum_{p=1}^N \mu_p (1 + \rho_p^2 \nu_p^2 \tau_p^2 G^2) \langle u_p w_p \rangle. \quad (\text{II-157})$$

Substituting this value into equation (II-155) and replacing  $D$  by  $\frac{kT}{f}$  yields

$$[\eta] = \frac{N_a kT}{2M\eta_s \delta} \sum_{p=1}^N \frac{1}{\lambda_p} \cdot \frac{1 + \rho_p^2 \nu_p^2 \tau_p^2 G^2}{1 + \rho_p \nu_p (2 + \rho_p \nu_p) \tau_p^2 G^2}. \quad (\text{II-158})$$

In the limiting case of zero velocity gradient, the intrinsic viscosity becomes

$$[\eta] = \frac{N_a b^2 f}{6M\eta_s} \sum_{p=1}^N \frac{1}{\lambda_p}, \quad (\text{II-159})$$

since  $G=0$  and  $\delta$  is given by equation (II-86) as  $3kT/b^2 f$ .

Thus the predicted value of the intrinsic viscosity at zero velocity gradient requires the evaluation of the eigenvalues  $\lambda_p$  of the matrix  $H \cdot A$ .

### The Calculation of Relaxation Times from Intrinsic Viscosity Data

The relaxation times defined by equation (II-154) may be written as

$$\tau_p = \frac{b^2 f}{6kT \lambda_p} \quad (\text{II-160})$$

by substituting the value of  $\delta$ . The longest, or "terminal," relaxation time  $\tau_1$ , corresponds to the smallest eigenvalue  $\lambda_1$ , and is associated with the stretching or contraction of the entire chain. The shortest relaxation time  $\tau_N$  corresponds to the largest eigenvalue  $\lambda_N$  and is associated with the 180 degrees out of phase motion of adjacent beads on the chain. As such,  $\tau_N$  should be almost constant for different molecular weight samples of the same polymer in solution, if the number of statistical segments is in direct proportion to the molecular weight of the polymer.

A value for the terminal relaxation time  $\tau_1$  may be obtained from knowledge of  $[\eta]$  and the eigenvalues  $\lambda_p$  without knowing the values of  $b^2$  and  $f$ . By equation (II-160),

$$\tau_1 = \frac{b^2 f}{6kT \lambda_1} \quad (\text{II-161})$$

But by equation (II-159)

$$\frac{b^2 f}{6} = \frac{[\eta] M \eta_s}{Na \sum_{p=1}^N \lambda_p} \quad (\text{II-162})$$

Thus

$$\tau_1 = \frac{[\eta] M \eta_s}{kT Na \lambda_1 \sum_{p=1}^N \lambda_p} \quad (\text{II-163})$$

Using a form advanced by Thurston (35), this may be written as

$$\tau_1 = C(N, h^*) \frac{[\eta] M \eta_s}{Na kT} \quad (\text{II-164})$$

where

$$C(N, h^*) = \left[ \sum_{p=1}^N \frac{\lambda_1}{\lambda_p} \right]^{-1}. \quad (\text{II-165})$$

This value of  $\tau_1$ , computed from steady flow intrinsic viscosity measurements, can be compared with experimentally determined values of  $\tau_1$  from independent oscillatory flow birefringence measurements on the same polymer samples.

Some differences should be expected in the two sets of values for  $\tau_1$ , since viscosity measurements are made under dilute solution conditions and the birefringence measurements are made at the higher concentration value of 3 percent by weight.

## CHAPTER III

### NUMERICAL EIGENVALUE CALCULATIONS AND RELATED FUNCTIONS

#### Preliminary Calculations

In order to obtain theoretical values for the intrinsic viscosity for the special case solution to the linear chain model considered in the previous chapter (i.e., low internal viscosity and zero velocity gradient limit), the eigenvalues  $\lambda_p$  of the matrix  $\mathbb{H} \cdot \mathbb{A}$  must be computed satisfying equation (II-91).

For the free-draining case of no hydrodynamic interaction, (i.e.,  $h^* = 0.0$ ), the free-draining eigenvalues are then simply the eigenvalues of the matrix  $\mathbb{A}$  and are exactly given by

$$\lambda_{p, \text{free}} = 4 \sin^2 \frac{p\pi}{2(N+1)} \quad . \quad (\text{III-1})$$

The exact details of this solution are given in chapter three of reference (34).

For the case of  $h^* \neq 0$ , the eigenvalues  $\lambda_p$  are not so easily evaluated. The eigenvalue equation to be solved is

$$(\mathbb{H} \cdot \mathbb{A}) \vec{\alpha}_p = \lambda_p \vec{\alpha}_p \quad (\text{III-2})$$

where the  $\vec{\alpha}_p$  are the eigenvectors of  $\mathbb{H} \cdot \mathbb{A}$ . This can be written as

$$(\mathbb{H} \cdot \mathbb{A}) \vec{\alpha}_p = \lambda_p \mathbb{1} \vec{\alpha}_p, \quad (\text{III-3})$$

or

$$(\mathbb{H} \cdot \mathbb{A} - \lambda_p \mathbb{1}) \vec{\alpha}_p = 0. \quad (\text{III-4})$$



This has a nontrivial solution only if

$$\det (\mathbb{H} \cdot \mathbb{A} - \lambda_p \mathbb{1}) = 0. \quad (\text{III-5})$$

Denoting the product of  $\mathbb{H}$  and  $\mathbb{A}$  by  $\mathbb{P}$ ,

$$\mathbb{P} = \mathbb{H} \cdot \mathbb{A}, \quad (\text{III-6})$$

then equation (III-5) may be written in determinant form as

$$\begin{vmatrix} P_{00} - \lambda & P_{01} & P_{02} & \dots & P_{0N} \\ P_{10} & P_{11} - \lambda & P_{12} & & P_{1N} \\ P_{20} & P_{21} & P_{22} - \lambda & & P_{2N} \\ \vdots & & & \ddots & \vdots \\ P_{N0} & P_{N1} & P_{N2} & \dots & P_{NN} - \lambda \end{vmatrix} = 0. \quad (\text{III-7})$$

This gives an  $(N+1)$ st order polynomial in  $\lambda$  and thus yields  $N+1$  roots. By the nature of  $\mathbb{H} \cdot \mathbb{A}$ , all the roots  $\lambda_p$  are real and non-negative. Negative or imaginary values of  $\lambda_p$  do not have physical meaning in the form in which they have been used.

As has been mentioned,  $\mathbb{H}$  and  $\mathbb{A}$  are both symmetric matrices, although  $\mathbb{H} \cdot \mathbb{A}$  is in general not symmetric. A consequence of the symmetry of  $\mathbb{H}$  and  $\mathbb{A}$  is that

$$P_{00} = P_{NN}$$

and

$$P_{jj} = P_{kk}, \quad j, k \neq 0, N. \quad (\text{III-8})$$

which forces one of the roots of  $\lambda$  to be zero. This root is labeled  $\lambda_0$  and is not used further. It corresponds to an infinite value of  $\tau_0$  for which the chain moves as a rigid body. The remainder of the calculated eigenvalues are labeled  $\lambda_1$  through  $\lambda_N$  in increasing order. Thus  $\lambda_1$  is the smallest nonzero eigenvalue and corresponds to the longest or terminal relaxation time  $\tau_1$ .

The solution for  $\lambda_p$  becomes quite involved if  $N$  is large, so approximations must generally be used. Pyun and Fixman (18) have developed an expression for  $\lambda_p$  for large  $N$  which, when cast in the form of the segmental hydrodynamic interaction factor  $h^*$ , has the form

$$\lambda_p \simeq 4 \sin^2 \frac{p\pi}{2(N+1)} + 4 h^* N^{3/2} [I_1(p) + I_2(p)], \quad (\text{III-9})$$

where the function  $[I_1(p) + I_2(p)]$  is as defined by Pyun and Fixman. For  $p > 20$  the function is approximated by

$$[I_1(p) + I_2(p)] \simeq p^{1/2} \pi \left[ \frac{p\pi}{2} - \frac{1}{4} \right]. \quad (\text{III-10})$$

Note that in the case of no hydrodynamic interaction ( $h^* = 0.0$ ) the expression in equation (III-9) reduces to equation (III-1) for the free-draining eigenvalues. The objection to using equation (III-9) is that it applies only for large  $N$  and for  $p \ll N$ . For small values of  $N$ , equation (III-9) gives values for  $\lambda_p$  which are consistently too large (compare Figures 2, 3, and 4) and therefore do not yield correct  $\lambda_p$ -dependent predictions from the theory. A computer program was written for the IBM 7040 that calculated values of  $\lambda_p$  for values of  $N$  from 1 to 1000 and for any value of  $h^*$ , using equation (III-9).

For the case of small  $N$ , fortunately, equation (III-7) may be solved exactly for the values of  $\lambda_p$ . As an example, the eigenvalues

for  $N=1$  and  $N=2$  will be calculated.

For the illustrative case of  $N=1$ , the Kirkwood-Riseman value for  $\langle \frac{1}{R_{jk}} \rangle$  will be used as given by equation (II-58). For  $|j-k|=1$ ,

$$\langle \frac{1}{R_{jk}} \rangle = \left( \frac{6}{\pi} \right)^{1/2} \frac{1}{l \cdot b} = \left( \frac{6}{\pi} \right)^{1/2} \frac{1}{b}. \quad (\text{III-11})$$

Then the matrix  $H$  is given by equation (II-83) as

$$H = \begin{pmatrix} 1 & \sqrt{2} h^* \\ \sqrt{2} h^* & 1 \end{pmatrix}. \quad (\text{III-12})$$

By equation (II-6),

$$A = \begin{pmatrix} 1 & -1 \\ -1 & 1 \end{pmatrix}. \quad (\text{III-13})$$

Therefore

$$H \cdot A = \begin{pmatrix} 1 - \sqrt{2} h^* & -1 + \sqrt{2} h^* \\ -1 + \sqrt{2} h^* & 1 - \sqrt{2} h^* \end{pmatrix}. \quad (\text{III-14})$$

The equation for  $\lambda$  in the form of equation (III-7) is then

$$\begin{vmatrix} 1 - \sqrt{2} h^* - \lambda & -1 + \sqrt{2} h^* \\ -1 + \sqrt{2} h^* & 1 - \sqrt{2} h^* - \lambda \end{vmatrix} = 0 \quad (\text{III-15})$$

which has roots

$$\begin{aligned} \lambda_0 &= 0 \\ \lambda_1 &= 2(1 - \sqrt{2} h^*) \end{aligned} \quad (\text{III-16})$$

This is the same numerical result that is obtained from the Zimm formalism (36).

For the following case of  $N=2$  the Treloar values of  $\langle \frac{1}{R_{jk}} \rangle$  will be used, although calculations for both the Kirkwood-Riseman and Treloar values for  $N=1$  to  $N=15$  have been made and are discussed later. Using the values of  $\langle \frac{1}{R_{jk}} \rangle$  given by equations (II-48) and (II-49),  $\mathbb{H}$  is given by

$$\mathbb{H} = \begin{pmatrix} 1 & 1.023 h^* & 1.023 h^* \\ 1.023 h^* & 1 & 1.023 h^* \\ 1.023 h^* & 1.023 h^* & 1 \end{pmatrix}. \quad (\text{III-17})$$

Also, for  $N=2$ ,

$$\mathbb{A} = \begin{pmatrix} 1 & -1 & 0 \\ -1 & 2 & -1 \\ 0 & -1 & 1 \end{pmatrix}. \quad (\text{III-18})$$

Thus

$$\mathbb{H} \cdot \mathbb{A} = \begin{pmatrix} 1-1.023 h^* & -1+1.023 h^* & 0 \\ -1+1.023 h^* & 2(1-1.023 h^*) & -1+1.023 h^* \\ 0 & -1+1.023 h^* & 1-1.023 h^* \end{pmatrix} \quad (\text{III-19})$$

and the equation for  $\lambda$  in the form of equation (III-7) is

$$\begin{vmatrix} 1-1.023 h^* - \lambda & -1+1.023 h^* & 0 \\ -1+1.023 h^* & 2(1-1.023 h^*) - \lambda & -1+1.023 h^* \\ 0 & -1+1.023 h^* & 1-1.023 h^* \end{vmatrix} = 0 \quad (\text{III-20})$$

The roots of this equation are

$$\lambda_0 = 0$$

$$\lambda_1 = 1 - 1.023 h^* \quad (\text{III-21})$$

$$\lambda_2 = 3 (1 - 1.023 h^*) .$$

### Eigenvalue Calculations

The above solutions are useful in that they provide a closed form solution for  $\lambda_1$  and  $\lambda_2$  in terms of  $h^*$ . For  $N=3$  and larger, however, this method becomes prohibitively cumbersome and numerical methods are used.

A program was written for an IBM 7040 computing system to compute values of  $\lambda_\rho$  for given values of  $N$  and  $h^*$  using both the Treloar and Kirkwood-Riseman expressions for  $\langle \frac{1}{R_{jk}} \rangle$ . Several programs are available from program libraries to compute eigenvalues of a real matrix. In computing the values for  $\lambda_\rho$  using the Treloar approximation to  $\langle \frac{1}{R_{jk}} \rangle$ , the Treloar values for  $\langle \frac{1}{R_{jk}} \rangle$  were actually used only from  $|j-k|=1$  to  $|j-k|=5$ . Beyond this value of  $|j-k|$  the Kirkwood-Riseman results were used to approximate the Treloar values since in this range the difference between the two occurs in the second and third decimal places. The convergence of the two values of  $\langle \frac{1}{R_{jk}} \rangle$  is illustrated by the following comparison of the first five terms of each series.

TABLE I  
COMPARISON OF KIRKWOOD-RISEMAN AND TRELOAR VALUES FOR  $\langle \frac{1}{R_{jk}} \rangle$

$ j-k $	Kirkwood-Riseman	Treloar
1	$\frac{1}{0.724b}$	$\frac{1}{b}$
2	$\frac{1}{1.023b}$	$\frac{1}{b}$
3	$\frac{1}{1.253b}$	$\frac{1}{1.333b}$
4	$\frac{1}{1.448b}$	$\frac{1}{1.500b}$
5	$\frac{1}{1.616b}$	$\frac{1}{1.669b}$

In the series of computer runs using the Kirkwood-Riseman approximations, the Kirkwood-Riseman values for  $\langle \frac{1}{R_{jk}} \rangle$  were, of course, used exclusively. Tables II - IV list the computer calculated eigenvalues for values of  $N$  from 1 to 15. In a few cases, eigenvalues were obtained for  $N=16$  as well. These are included in the tables also. Table II lists eigenvalues for the free-draining case (i.e.,  $h^*=0.0$ ) which are calculated using equation (III-1). From equation (III-1) the free-draining eigenvalues are located between the limits of 0.0 and 4.0. For every value of  $N$ , there are  $N$  nonzero eigenvalues, listed in order in the table from  $\lambda_1$  to  $\lambda_N$ . Tables III and IV list the eigenvalues calculated using the Treloar and Kirkwood-

TABLE II  
FREE-DRAINING EIGENVALUES

EIGENVALUES FOR FREE-DRAINING CASE (HSTAR = 0.00)

N = 1								
2.0000								
N = 2								
1.0000	3.0000							
N = 3								
0.5858	2.0000	3.4142						
N = 4								
0.3820	1.3820	2.6180	3.6180					
N = 5								
0.2679	1.0000	2.0000	3.0000	3.7321				
N = 6								
0.1981	0.7530	1.5550	2.4450	3.2470	3.8019			
N = 7								
0.1522	0.5858	1.2346	2.0000	2.7654	3.4142	3.8478		
N = 8								
0.1206	0.4679	1.0000	1.6527	2.3473	3.0000	3.5321	3.8794	
N = 9								
0.0979	0.3820	0.8244	1.3820	2.0000	2.6180	3.1756	3.6180	
3.9021								
N = 10								
0.0810	0.3175	0.6903	1.1692	1.7154	2.2846	2.8308	3.3097	
3.6825	3.9190							
N = 11								
0.0681	0.2679	0.5858	1.0000	1.4824	2.0000	2.5176	3.0000	
3.4142	3.7321	3.9319						
N = 12								
0.0581	0.2291	0.5030	0.8639	1.2908	1.7589	2.2411	2.7092	
3.1361	3.4970	3.7709	3.9419					
N = 13								
0.0501	0.1981	0.4363	0.753	1.1322	1.5550	2.0000	2.4450	
2.8678	3.2470	3.5637	3.8019	3.9499				
N = 14								
0.0437	0.1729	0.3820	0.6617	1.0000	1.3820	1.7909	2.2091	
2.6180	3.0000	3.3383	3.6180	3.8271	3.9563			
N = 15								
0.0384	0.1522	0.3371	0.5858	0.8889	1.2346	1.6098	2.0000	
2.3902	2.7654	3.1111	3.4142	3.6629	3.8478	3.9616		

TABLE III  
TRELOAR EIGENVALUES

## EIGENVALUES FROM TRELOAR DISTRIBUTION

HSTAR = 0.01

N = 1 1.980									
N = 2 0.990	2.969								
N = 3 0.581	1.977	3.381							
N = 4 0.380	1.367	2.588	3.584						
N = 5 0.267	0.990	1.976	2.967	3.698					
N = 6 0.198	0.747	1.537	2.416	3.212	3.768				
N = 7 0.153	0.582	1.221	1.976	2.733	3.379	3.814			
N = 8 0.121	0.466	0.990	1.633	2.319	2.966	3.4960	3.846		
N = 9 0.099 3.869	0.381	0.818	1.366	1.975	2.586	3.140	3.582		
N = 10 0.082 3.647	0.317 3.886	0.665	1.157	1.695	2.256	2.797	3.274		
N = 11 0.069 3.378	0.268 3.697	0.582 3.899	0.990	1.465	1.975	2.487	2.965		
N = 12 0.0589 3.1007	0.2295 3.4609	0.5007 3.7359	0.8565 3.9091	1.2767	1.7373	2.2131	2.6765		
N = 13 0.0509 2.8337	0.1987 3.2111	0.4347 3.5275	0.7473 3.7673	1.1207 3.9173	1.5365	1.9749	2.4147		
N = 14 0.0445 2.5859	0.1737 2.9651	0.3811 3.3021	0.6573 3.5821	0.9905 3.7927	1.3663 3.9237	1.7687	2.1813		
N = 15 0.0391 2.3601	0.1530 2.7319	0.3365 3.0754	0.5823 3.3777	0.8811 3.6269	1.2213 3.8134	1.5903 3.9290	1.9747		

HSTAR = 0.1

N = 1 1.795								
N = 2 0.898	2.693							
N = 3 0.539	1.770	3.078						
N = 4 0.361	1.230	2.315	3.276					
N = 5 0.260	0.903	1.760	2.664	3.390				
N = 6 0.197	0.692	1.374	2.151	2.897	3.462			
N = 7 0.155	0.548	1.102	1.755	2.439	3.059	3.510		
N = 8 0.126	0.445	0.904	1.455	2.058	2.656	3.175	3.544	
N = 9 0.104 3.569	0.370	0.755	1.225	1.752	2.301	2.822	3.262	
N = 10 0.088 3.328	0.312 3.588	0.640	1.047	1.506	2.000	2.495	2.951	
N = 11 0.075 3.052	0.267 3.380	0.550 3.602	0.904	1.309	1.750	2.207	2.652	
N = 12 0.0655 2.7807	0.2321 3.1345	0.4785 3.4211	0.7897 3.6135	1.1481	1.5419	1.9595	2.3809	
N = 13 0.0575 2.5267	0.2035 2.8867	0.4199 3.2015	0.6955 3.4545	1.0155 3.6227	1.3691	1.7481	2.1403	
N = 14 0.0510 2.2960	0.1800 2.6498	0.3718 2.9750	0.6174 3.2570	0.90480 3.4820	1.2240 3.6302	1.5682	1.9300	
N = 15 0.0455 2.0898	0.1604 2.4304	0.3315 2.7546	0.5517 3.0494	0.8113 3.3032	1.1010 3.5046	1.4143 3.6461	1.7469	
N = 16 0.0409 1.9072	0.1442 2.2306	0.2978 2.5469	0.4963 2.8444	0.7316 3.1127	0.9958 3.3424	1.2825 3.5238	1.5880 3.6412	



TABLE III. (continued)

## EIGENVALUES FROM TRELOAR DISTRIBUTION

HSTAR = 0.3

N = 1  
1.3862N = 2  
0.6931 2.0793N = 3  
0.444 1.309 2.406N = 4  
0.319 0.924 1.709 2.593N = 5  
0.245 0.707 1.279 1.993 2.707N = 6  
0.195 0.569 1.011 1.561 2.198 2.783N = 7  
0.161 0.473 0.835 1.263 1.787 2.349 2.836N = 8  
0.135 0.400 0.710 1.058 1.480 1.969 2.462 2.875N = 9  
0.116 0.345 0.616 0.911 1.253 1.666 2.115 2.551  
2.904N = 10  
0.101 0.301 0.541 0.800 1.086 1.430 1.824 2.233  
2.620 2.926N = 11  
0.089 0.266 0.480 0.713 0.960 1.247 1.586 1.957  
2.330 2.676 2.943N = 12  
0.0798 0.2374 0.4292 0.6410 0.8618 1.1064 1.3954 1.7240  
2.0702 2.4104 2.7224 2.9574N = 13  
0.0718 0.2136 0.3870 0.5804 0.7816 0.9958 1.2430 1.5302  
1.8444 2.1666 2.4780 2.7606 2.9688N = 14  
0.0650 0.1935 0.3510 0.5285 0.7142 0.9067 1.1208 1.3705  
1.6516 1.9497 2.2491 2.5356 2.7925 2.9779N = 15  
0.0593 0.1765 0.3205 0.4838 0.6561 0.833 1.0222 1.2397  
1.4886 1.7605 2.0419 2.3206 2.5849 2.8195 2.9856

HSTAR = 0.4

N = 1  
1.1816N = 2  
0.5908 1.7724N = 3  
0.3957 1.0792 2.0698N = 4  
0.2981 0.7704 1.4058 2.2519N = 5  
0.2370 0.6083 1.0370 1.6588 2.3667N = 6  
0.1942 0.5074 0.8281 1.2652 1.8499 2.4444N = 7  
0.1631 0.4346 0.7006 1.0162 1.4617 1.9951 2.4997N = 8  
0.1399 0.3777 0.6131 0.8578 1.1900 1.6263 2.1072 2.5405N = 9  
0.1219 0.3321 0.5461 0.7524 1.0032 1.3489 1.7619 2.1960  
2.5714N = 10  
0.1077 0.2951 0.4911 0.6765 0.8752 1.1440 1.4885 1.8748  
2.2673 2.5953N = 11  
0.09613 0.2648 0.4444 0.6168 0.7849 0.9953 1.2757 1.6100  
1.9692 2.3256 2.6143N = 12  
0.08657 0.2395 0.4045 0.5666 0.7177 0.8874 1.1129 1.3957  
1.7154 2.0490 2.3739 2.6295N = 13  
0.07856 0.2181 0.3703 0.5229 0.6641 0.8079 0.9895 1.2251  
1.5036 1.8070 2.1170 2.4143 2.6419N = 14  
0.07177 0.1999 0.3406 0.4841 0.6187 0.7472 0.8962 1.0906  
1.3296 1.6001 1.8868 2.1756 2.4485 2.6520N = 15  
0.06593 0.1842 0.3148 0.4498 0.5785 0.6984 0.8250 0.9853  
1.1879 1.4258 1.6861 1.9568 2.2264 2.4776 2.6605

TABLE IV  
KIRKWOOD-RISEMAN EIGENVALUES

EIGENVALUES FROM KIRKWOOD-RISEMAN APPROXIMATION

HSTAR = 0.01

N = 1  
1.9717

N = 2  
0.9899    2.9534

N = 3  
0.5822    1.9740    3.3589

N = 4  
0.3809    1.3675    2.5799    3.5583

N = 5  
0.2681    0.9920    1.9745    2.9540    3.6697

N = 6  
0.1988    0.7488    1.5380    2.4108    3.1956    3.7380

N = 7  
0.1532    0.5838    1.2255    1.9748    2.7245    3.3592    3.7828

N = 8  
0.1217    0.4673    0.9925    1.6342    2.3153    2.9542    3.4744    3.8137

N = 9  
0.0990    0.3822    0.8196    1.3684    1.9750    2.5805    3.1259    3.5584  
3.8359

N = 10  
0.0821    0.3183    0.6873    1.1593    1.6959    2.2540    2.7887    3.2571  
3.6214    3.8524

N = 11  
0.0693    0.2691    0.5842    0.9928    1.4672    1.9752    2.4823    2.9543  
3.3593    3.6698    3.8650

N = 12  
0.0592    0.2305    0.5023    0.8588    1.2790    1.7388    2.2115    2.6698  
3.0874    3.4402    3.7078    3.8748

N = 13  
0.0512    0.1996    0.4364    0.7495    1.1231    1.5386    1.9752    2.4113  
2.8250    3.1958    3.5053    3.7381    3.8826

N = 14  
0.0447    0.1746    0.3826    0.6594    0.9930    1.3687    1.7703    2.1832  
2.5806    2.9543    3.2851    3.5584    3.7627    3.8888

N = 15  
0.0394    0.1539    0.3380    0.5844    0.8835    1.2239    1.5925    1.9753  
2.3576    2.7248    3.0630    3.3593    3.6023    3.7828    3.8940

N = 16  
0.0350    0.1368    0.3008    0.5214    0.7908    1.0999    1.4383    1.7944  
2.1562    2.5114    2.8482    3.1551    3.4217    3.6389    3.7996    3.8983

HSTAR = 0.1

N = 1  
1.7171

N = 2  
0.8999    2.5343

N = 3  
0.5499    1.7402    2.8613

N = 4  
0.3721    1.2380    2.2375    3.0207

N = 5  
0.2699    0.9206    1.7457    2.5402    3.1093

N = 6  
0.2055    0.7108    1.3855    2.1036    2.7338    3.1634

N = 7  
0.1624    0.5660    1.1220    1.7489    2.3576    2.8642    3.1987

N = 8  
0.1319    0.4620    0.9258    1.4685    2.0277    2.5422    2.9557    3.2231

N = 9  
0.1096    0.3848    0.7768    1.2470    1.7507    2.2427    2.6796    3.0222  
3.2406

N = 10  
0.0927    0.3260    0.6614    1.0707    1.5212    1.9791    2.4105    2.7841  
3.0719    3.2535

N = 11  
0.0796    0.2801    0.5702    0.9288    1.3312    1.7520    2.1643    2.5432  
2.8652    3.1101    3.2634

N = 12  
0.0692    0.2435    0.4970    0.8133    1.1735    1.5578    1.9454    2.3156  
2.6497    2.9293    3.1399    3.2711

N = 13  
0.0608    0.2140    0.4374    0.7182    1.0416    1.3919    1.7529    2.1076  
2.4401    2.7361    2.9807    3.1638    3.2773

N = 14  
0.0539    0.1897    0.3882    0.6391    0.9305    1.2500    1.5845    1.9206  
2.2443    2.5438    2.8070    3.0226    3.1832    3.2822

N = 15  
0.0482    0.1694    0.3471    0.5726    0.8362    1.1282    1.4375    1.7536  
2.0647    2.3603    2.6306    2.8659    3.0570    3.1991    3.2862

N = 16  
0.0434    0.1524    0.3124    0.5161    0.7556    1.0230    1.3090    1.6050  
1.9016    2.1890    2.4592    2.7040    2.9152    3.0858    3.2123    3.2896

TABLE IV (continued)

EIGENVALUES FROM KIRKWOOD-RIESEN APPROXIMATION

HSTAR = 0.3

N = 1  
1.1515N = 2  
0.7000 1.6029N = 3  
0.4774 1.2207 1.7563N = 4  
0.3514 0.9499 1.4778 1.8267N = 5  
0.2724 0.7610 1.2381 1.6215 1.8642N = 6  
0.2192 0.6255 1.0474 1.4217 1.7083 1.8866N = 7  
0.1813 0.5252 0.8970 1.2477 1.5431 1.7648 1.9009N = 8  
0.1533 0.4489 0.7775 1.1008 1.3894 1.6276 1.8034 1.9107N = 9  
0.1318 0.3892 0.6814 0.9774 1.2531 1.4930 1.6883 1.8309  
1.9177N = 10  
0.1149 0.3417 0.6032 0.8739 1.1336 1.3690 1.5706 1.7334  
1.8544 1.9228N = 11  
0.1014 0.3031 0.5385 0.7865 1.0295 1.2569 1.4585 1.6304  
1.7678 1.8664 1.9267N = 12  
0.0904 0.2712 0.4846 0.7121 0.9392 1.1561 1.3548 1.5290  
1.6773 1.7943 1.9783 1.9298N = 13  
0.0812 0.2446 0.4390 0.6484 0.8605 1.0664 1.2594 1.4336  
1.5855 1.7148 1.8152 1.8878 1.9322N = 14  
0.0735 0.2220 0.4001 0.5934 0.7916 0.9866 1.1723 1.3443  
1.4977 1.6318 1.7450 1.8320 1.8955 1.9341N = 15  
0.0670 0.2020 0.366 0.5458 0.731 0.9158 1.0936 1.2616  
1.40 1.54 1.63 1.72 1.80 1.87 1.94

HSTAR = 0.4

N = 1  
0.8686N = 2  
0.6000 1.1372N = 3  
0.4397 0.9609 1.2051N = 4  
0.3393 0.8047 1.0996 1.2307N = 5  
0.2719 0.6795 0.9851 1.1638 1.2425N = 6  
0.2244 0.5809 0.8782 1.0820 1.1971 1.2488N = 7  
0.1894 0.5028 0.7839 0.9977 1.1374 1.2164 1.2525N = 8  
0.1627 0.4404 0.7023 0.9170 1.0714 1.1716 1.2283 1.2549N = 9  
0.1418 0.3896 0.6326 0.8423 1.0049 1.1194 1.1939 1.2362  
1.2565N = 10  
0.1251 0.3478 0.5728 0.7748 0.9400 1.0649 1.1519 1.2093  
1.2415 1.2577N = 11  
0.1114 0.3130 0.5214 0.7145 0.8786 1.0098 1.1067 1.1751  
1.2201 1.2452 1.2586N = 12  
0.1001 0.2836 0.4770 0.6605 0.8218 0.9554 1.0604 1.1368  
1.1921 1.2278 1.2480 1.2593N = 13  
0.09069 0.2585 0.4385 0.6124 0.7694 0.9036 1.0131 1.0976  
1.1593 1.2051 1.2334 1.2502 1.2598N = 14  
0.08265 0.2369 0.4048 0.5695 0.7215 0.8547 0.9665 1.0569  
1.1255 1.1767 1.2149 1.2375 1.2520 1.2602N = 15  
0.07573 0.2182 0.3751 0.5313 0.6774 0.8090 0.9214 1.0158  
1.0903 1.1470 1.1905 1.2225 1.2406 1.2535 1.2605

Riseman approximations respectively. In each case, sets of eigenvalues are given using values of  $h^* = 0.01, 0.1, 0.3, \text{ and } 0.4$  as parameters.

As an aid in comparing the different sets of eigenvalues, Figures 1 through 4 show graphs of  $\lambda_p$  versus  $N$  for the free-draining case and for the Pyun-Fixman, Treloar, and Kirkwood-Riseman cases, using  $h^* = 0.1$  as the parameter. All eigenvalues are shown from  $N=1$  to  $N=15$  and on the free-draining and Pyun-Fixman plots every tenth eigenvalue (i.e.,  $\lambda_{10}, \lambda_{20}, \lambda_{30}, \dots$ ) is shown through  $N=100$ . The approach of the  $\lambda_N$  values to 4.0 in the free-draining case is matched by similar asymptotic conditions in the other three figures. The upper bounds are not the same for each case, however, since the Pyun-Fixman asymptote is about 6.0, the Treloar value is about 3.7, and the Kirkwood-Riseman value is about 3.4. Since the Pyun-Fixman eigenvalues are developed using the assumption that  $N$  is large and using the Kirkwood-Riseman approximation of equation (II-58) (18), the plots of the Kirkwood-Riseman eigenvalues should be expected to approach the Pyun-Fixman values for large values of  $N$ , but a comparison of the two plots by superposition indicates that the convergence is very slow, if it indeed exists. Convergence of the two values of  $\lambda_p$  for values of  $p$  near  $N$  is not to be expected, even for large  $N$ , because the Pyun-Fixman expression is good only for values of  $p \ll N$ . Although the curves are only shown for one value of  $h^*$ , the envelope of the curves shifts downward along the  $\lambda_p$  axis as  $h^*$  is increased. The shift is only a general one, however, and is not so simple as to allow a simple empirical expression to be developed giving  $\lambda_p$  as a function of  $N$  and  $h^*$ .

Figure 1.  $\lambda_p$  Versus  $N$  for the Free-draining Case.

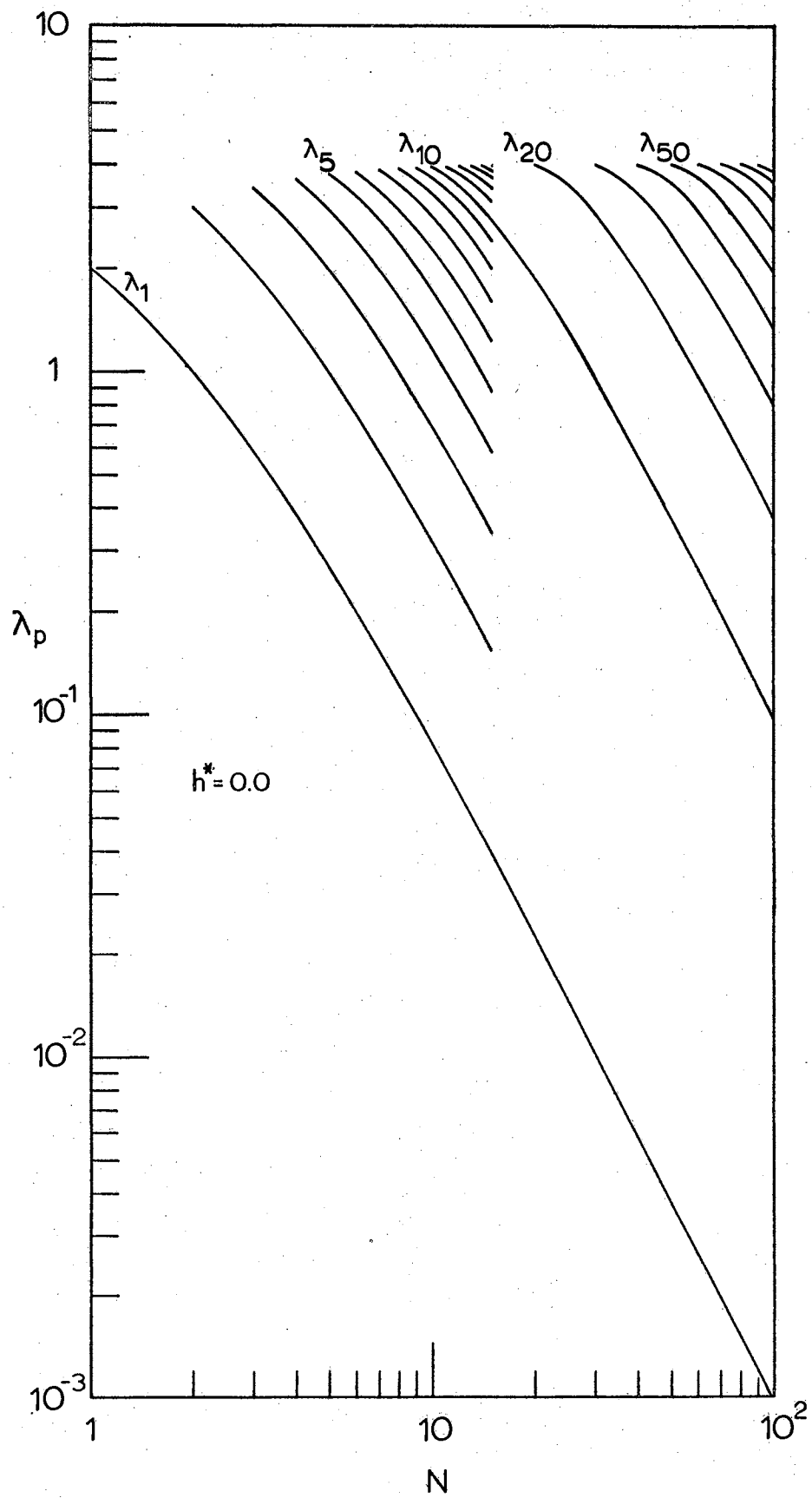


Figure 2. Pyun and Fixman Values of  $\lambda_p$  Versus  $N$   
for  $h^* = 0.1$ .

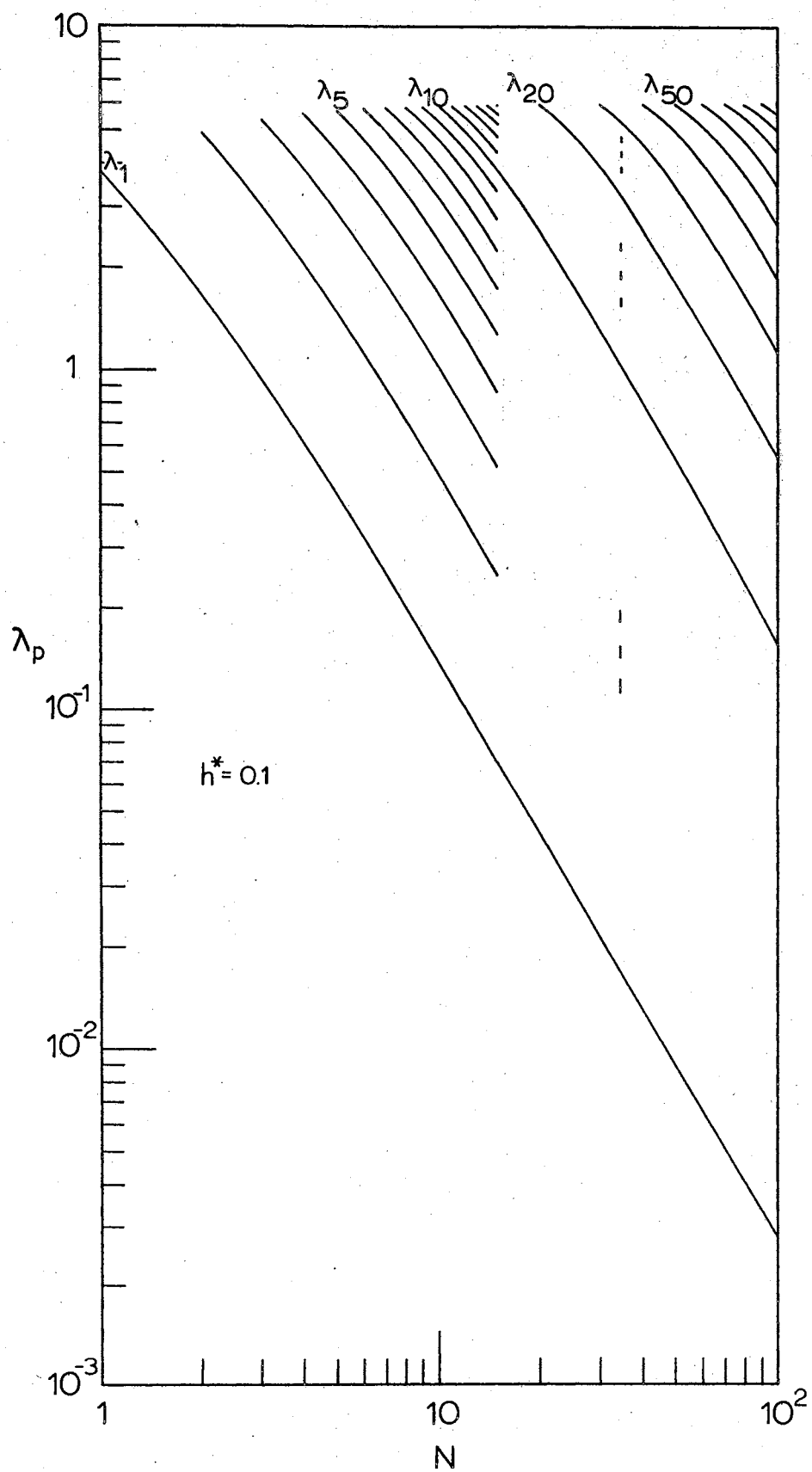




Figure 3. Treloar Values of  $\lambda_p$  Versus  $N$  for  $h^* = 0.1$ .

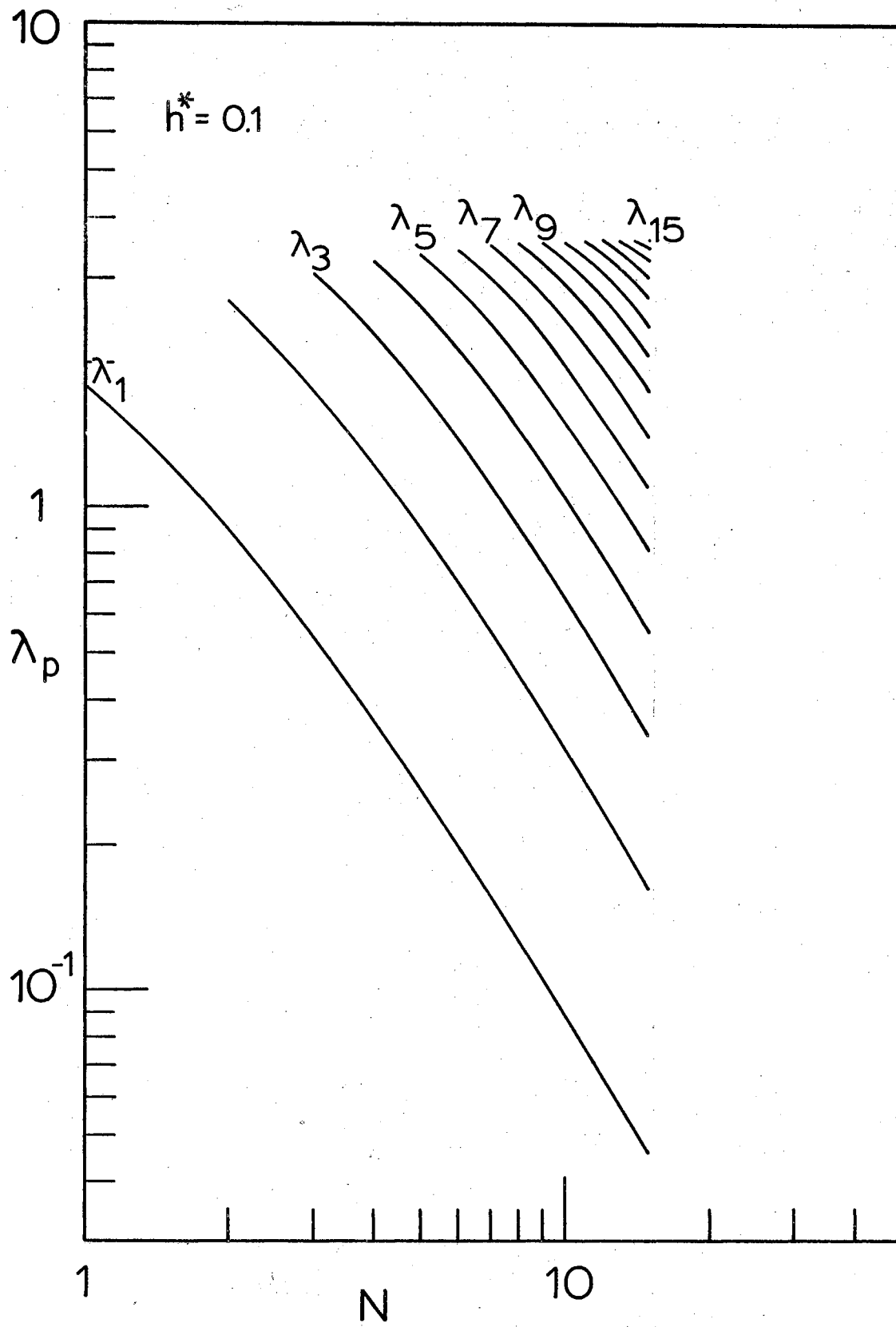
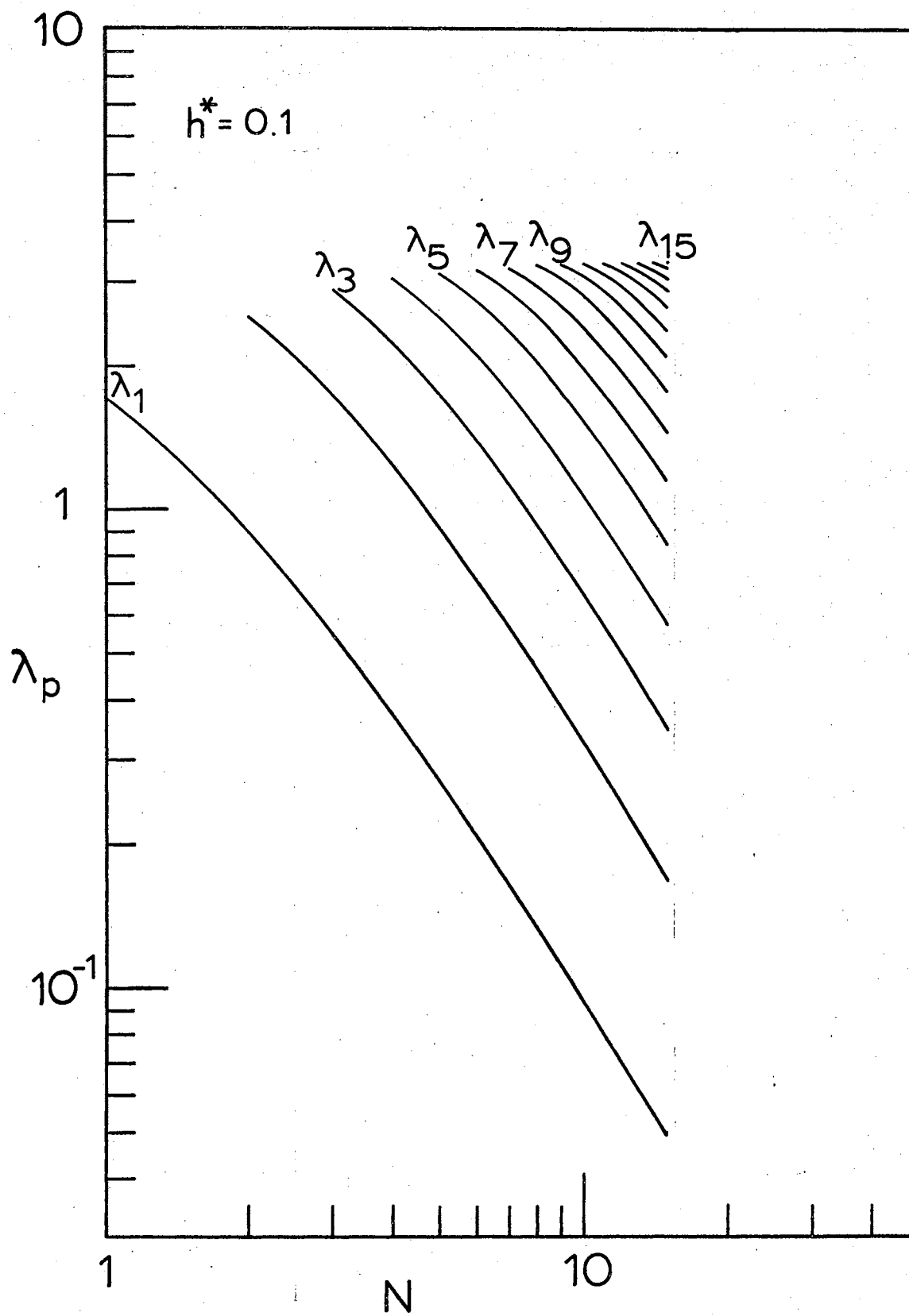


Figure 4. Kirkwood-Riseman Values of  $\lambda_p$  Versus  $N$   
for  $h^*=0.1$ .



### Calculation of Eigenvalue Dependent Functions

In order to examine the dependence of  $[\eta]$ , the intrinsic viscosity, upon  $M$ , the molecular weight, Thurston (19) has cast the expression for  $[\eta]$  given by equation (II-159) in the form

$$[\eta] = \phi N^{1/2} \frac{b^3}{N_a m_s}, \quad (\text{III-22})$$

where  $b$  is the segment length,  $N_a$  is Avogadro's number, and  $m_s$  is the segment mass. From the expression for  $h^*$  given in equation (II-66),

$$\frac{f}{6\eta_s} = \pi h^* b \left(\frac{\pi}{3}\right)^{1/2}, \quad (\text{III-23})$$

where  $f$  is the segmental friction factor and  $\eta_s$  is the solvent viscosity. Also  $m_s$  and  $M$  are related by

$$M = N(N_a m_s) \quad (\text{III-24})$$

Using equations (II-159), (III-23), and (III-24), can be written as

$$[\eta] = \left(\frac{b^3}{N_a m_s}\right) \cdot \frac{N_a \pi^{3/2}}{3^{1/2}} \cdot \frac{h^*}{N^{1/2}} \cdot N^{1/2} \sum_{p=1}^N \frac{1}{\lambda_p}, \quad (\text{III-25})$$

which is of the form of equation (III-22) where

$$\phi = \frac{N_a \pi^{3/2}}{3^{1/2}} \cdot \frac{h^*}{N^{1/2}} \sum_{p=1}^N \frac{1}{\lambda_p}. \quad (\text{III-26})$$

The function  $\phi N^{1/2}$  is thus useful to compare against values of  $[\eta]$ , since they differ only by the factor  $b^3/N_a m_s$ , which is constant for different molecular weight samples of the same polymer in the same solvent, assuming that  $N$  is directly proportional to  $M$  according to equation (III-24). Plots of  $\phi N^{1/2}$  versus  $N$  should thus exhibit the same character as  $[\eta]$  versus  $M$  plots. Figures 5 through 7 show

$\phi N^{1/2}$  plotted against  $N$  for  $h^*$  values of 0.01, 0.1, 0.3, and 0.4. The values for  $h^* = 0.05, 0.15,$  and  $0.2$  on Figure 6 were not calculated, but were geometrically interpolated from the curves for other values.

The deciding factor on whether to use the Treloar or the Kirkwood-Riseman eigenvalues is their ability to predict the character of the observed  $[\eta]$ ,  $M$  dependence for low molecular weights. The upward turn of the plot of  $[\eta]$  versus  $M$  for polystyrene in Aroclor 1248 for low molecular weights shown in Figure 10 is typical of the results observed with other polymers. Several examples of this effect are given in the next chapter. The plots of  $\phi N^{1/2}$  versus  $N$  calculated from the Treloar eigenvalues do not have this character, but the  $\phi N^{1/2}$  versus  $N$  plots from the Kirkwood-Riseman eigenvalues do. For this reason, only the Kirkwood-Riseman results will be used to compare with intrinsic viscosity measurements in the next chapter.

The problem of the convergence of the Pyun-Fixman and Kirkwood-Riseman  $\phi N^{1/2}$  versus  $N$  plots reappears at this point. Overlaying the two plots to obtain comparisons, the Pyun-Fixman and the Kirkwood-Riseman curves are almost identical for low values of  $h^*$ , but for values of  $h^* = 0.3$  and  $0.4$ , the convergence, if it occurs, must be for values of  $N$  on the order of  $10^4$ . A set of extrapolated values for the Kirkwood-Riseman curves which approach the Pyun-Fixman curves for large values of  $N$  can be used in comparing measured  $[\eta]$  versus  $M$  curves with theoretical plots of  $\phi N^{1/2}$  versus  $N$  by superposition. The inaccuracy, however, of the Pyun-Fixman values of  $\lambda_p$  for values of  $p$  near  $N$  may mean that such an extrapolation is invalid and that convergence does not occur.

Figure 5.  $\phi N^k$  Versus  $N$  Using Treloar Eigenvalues.

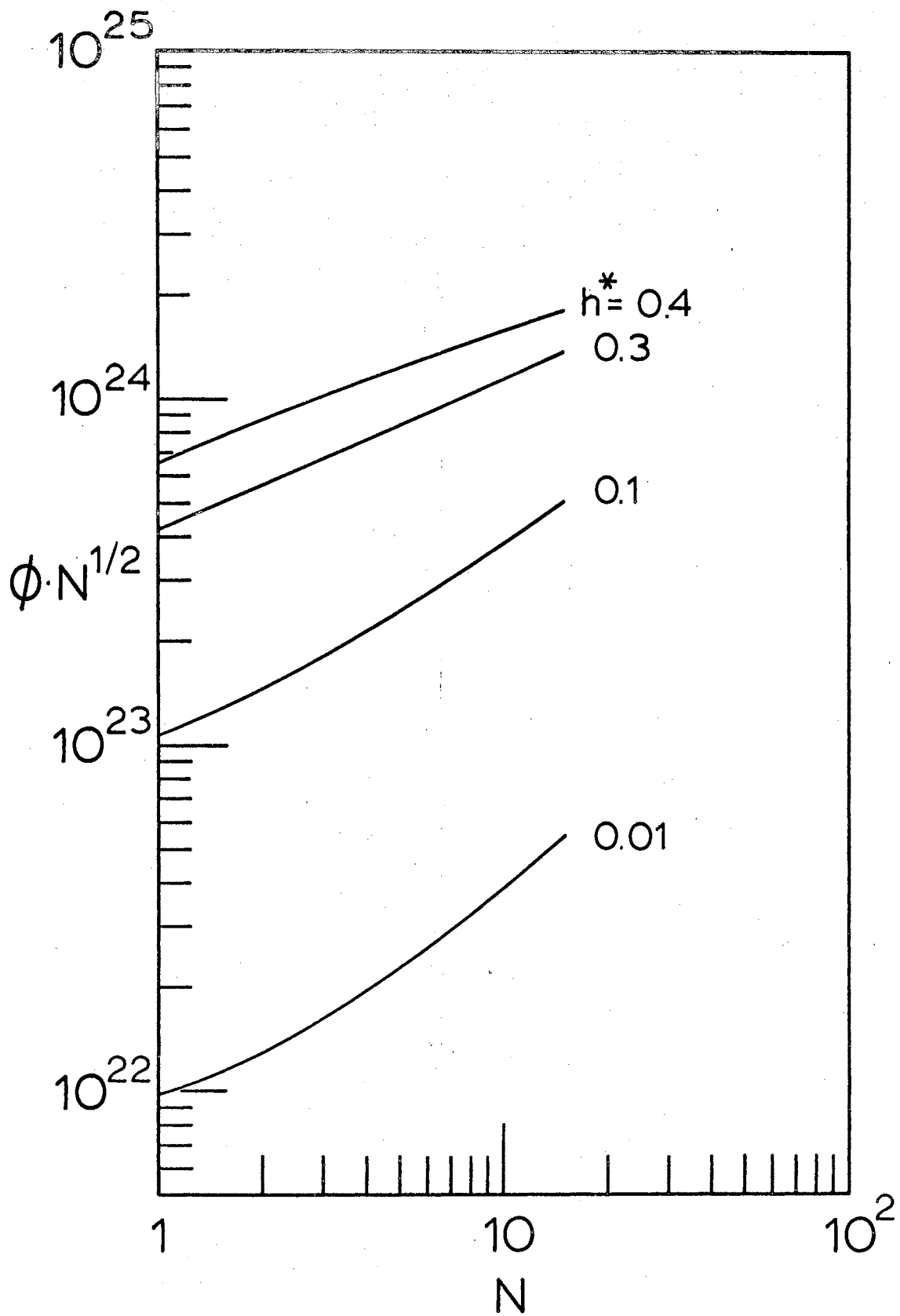




Figure 6.  $\phi N^k$  Versus  $N$  Using Kirkwood-Riseman  
Eigenvalues.

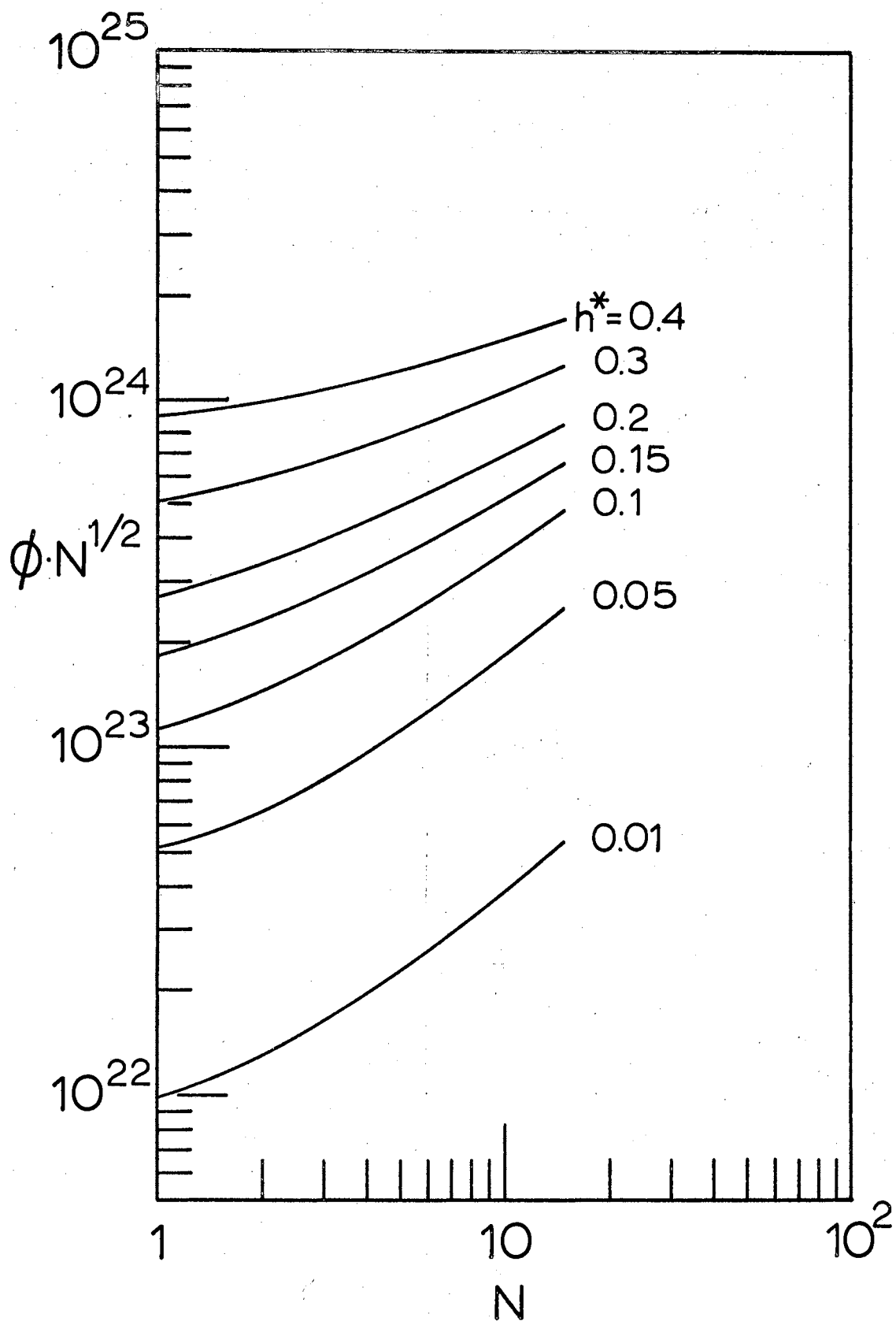


Figure 7.  $\phi N^{1/2}$  Versus  $N$  Using Pyun and Fixman Eigenvalues.

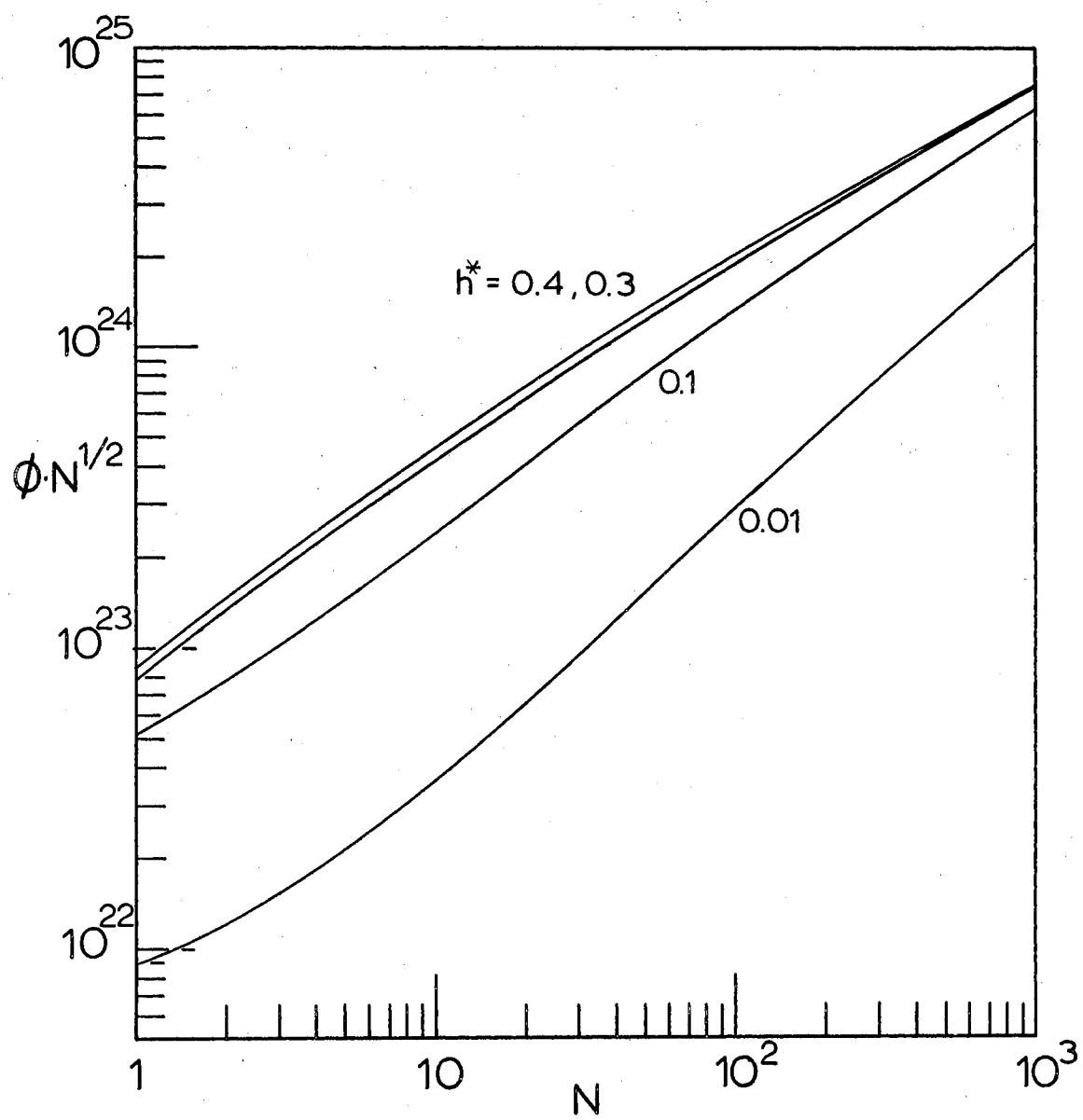


Figure 8.  $C(N, h^*)$  Versus  $N$  Using Kirkwood-Riseman Eigenvalues.

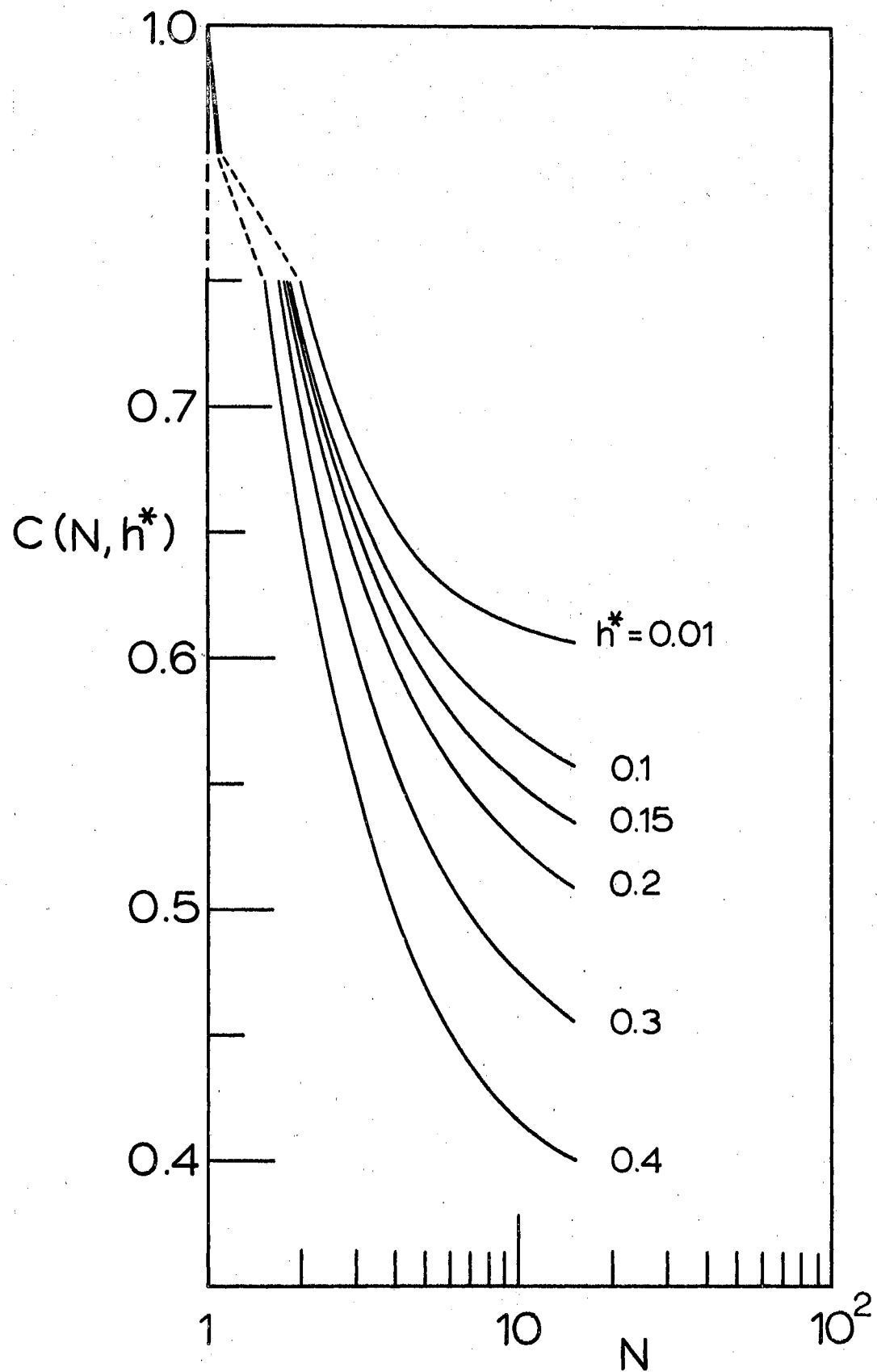
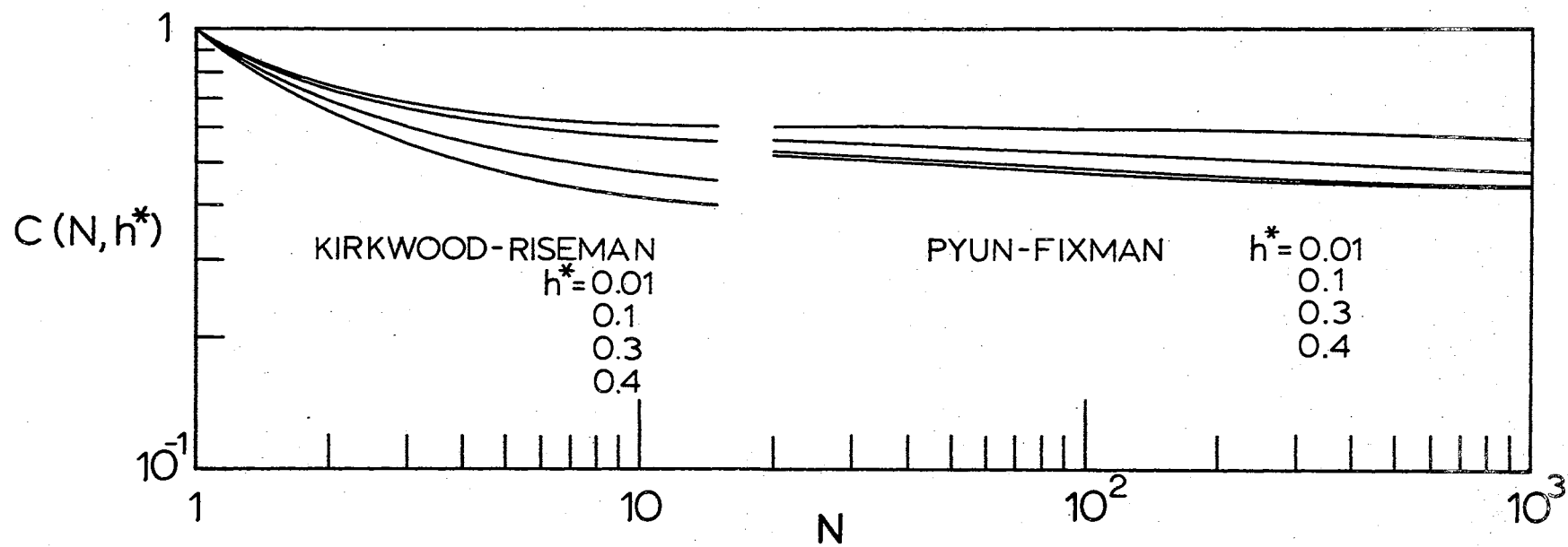


Figure 9. Comparison of  $C(N, h^*)$  Versus  $N$  Calculated  
From Kirkwood-Riseman and Pyun and Fixman  
Eigenvalues.





The  $C(N, h^*)$  function used to derive terminal relaxation times from intrinsic viscosity measurements and given by equation (II-165) is shown plotted against  $N$  in Figure 8, using the Kirkwood-Riseman eigenvalues only. The curves for  $h^*$  values of 0.01, 0.1, 0.3, and 0.4 are calculated, but the curves for  $h^* = 0.15$  and  $h^* = 0.2$  are interpolated geometrically. The use of the figure is explained in detail in the calculations of the following chapter. The problem of the convergence of the values of the  $C(N, h^*)$  function calculated from the Kirkwood-Riseman eigenvalues with those calculated from the Pyun-Fixman eigenvalues is illustrated in Figure 9. The Kirkwood-Riseman eigenvalues are used for  $N = 1$  to  $N = 15$  and the Pyun-Fixman eigenvalues are used from  $N = 20$  to  $N = 1000$ . Again, the higher values of  $h^*$  produce curves which do not appear to converge for large values of  $N$ . The general problem of convergence as discussed in this chapter will be partially resolved with more extensive calculations of exact eigenvalues for values of  $N$  higher than 15.

## CHAPTER IV

### COMPARISON WITH MEASUREMENTS

#### Polystyrene in Aroclor 1248

The predicted behavior of the intrinsic viscosity of low molecular weight polymers in solution can be compared with actual data by comparing the plots of  $\phi N^{1/2}$  versus  $N$  with experimental plots of  $[\eta]$  versus  $M$ . Since

$$[\eta] = \phi N^{1/2} \frac{b^2}{N a m_s} \quad , \quad (\text{IV-1})$$

where

$$\phi = \frac{N a \pi^{3/2}}{3^{1/2}} \cdot \frac{h^*}{N^{3/2}} \sum_{p=1}^N \frac{1}{\lambda_p} \quad , \quad (\text{IV-2})$$

values of  $[\eta]$  can be obtained from  $\phi N^{1/2}$  by specifying values for  $h^*$ ,  $b$ , and  $m_s$ . This procedure may be carried out in reverse by making a best fit of the  $\phi N^{1/2}$  versus  $N$  curves with the experimental  $[\eta]$  versus  $M$  curves. Figure 10 shows a plot of intrinsic viscosity versus molecular weight obtained by Thurston and Schrag (19) for dilute solutions of polystyrene in Aroclor 1248 over a wide range of molecular weights. The measurements were made at a temperature of 25°C, at which the viscosity of the Aroclor 1248 was 2.23 poises.

The dashed line through the data points shows clearly the characteristic upward curvature of the plot for low molecular weights. This characteristic of the curve shapes is also evident in the polystyrene

plots of Figure 13 and in the three polymers presented in Figure 14. As has been previously mentioned, the plots of  $\phi N^{1/2}$  versus  $N$  have this characteristic shape for low  $N$  (and therefore, low  $M$ ) only if the eigenvalues derived from the Kirkwood-Riseman expression of equation (II-58) are used to calculate the function  $\phi N^{1/2}$ . The plots of  $\phi N^{1/2}$  using the Treloar eigenvalues appear to approach the same values for high values of  $N$  that the Kirkwood-Riseman derived  $\phi N^{1/2}$  approach, but they do not have the proper character for low values of  $N$ . For the value of  $h^* = 0.3$ , the line even possesses a downward curvature for low  $N$ , in contrast to the upward turn of the experimental  $[\eta]$  versus  $M$  curves. The plots of  $\phi N^{1/2}$  calculated from the Pyun and Fixman eigenvalues also lack the character exhibited by the experimental  $[\eta]$  versus  $M$  plots for low molecular weights. The convergence of the  $\phi N^{1/2}$  curves from the Pyun and Fixman and from the Kirkwood-Riseman eigenvalues is slow, if indeed there is to be convergence for high  $N$  values, as discussed in chapter three. For these reasons, only the results from the Kirkwood-Riseman sets of eigenvalues are used in the remaining calculations of this section.

The solid line of Figure 10 is the theoretical curve of  $\phi N^{1/2}$  versus  $N$  for an  $h^*$  value of 0.15 and for a superposition of the theoretical and experimental curves such that  $N=1$  at  $M=3200$  and  $\phi N^{1/2} = 10^{24}$  at  $[\eta] = 43 \frac{\text{cm}^3}{\text{g}}$ . The theoretical curve for  $h^* = 0.15$  was interpolated from a plot of  $\phi N^{1/2}$  versus  $N$  for  $h^*$  values of 0.01, 0.1, 0.3 and 0.4.

Using the expressions

$$\eta_s = \frac{M}{N \cdot N_a} \quad , \quad (\text{IV-3})$$

$$b = \left[ \frac{[\eta] N_a m_s}{\phi N^{1/2}} \right]^{1/3}, \quad (\text{IV-4})$$

and

$$f = (12\pi^3)^{1/2} \eta_s b h^* \quad (\text{IV-5})$$

the following values are calculated:

$$m_s = 5.31 \times 10^{-21} \text{ g}, \quad (\text{IV-6})$$

$$b = 5.16 \times 10^{-7} \text{ cm}, \quad (\text{IV-7})$$

$$f = 3.33 \times 10^{-6} \text{ g} \cdot \text{sec}^{-1}. \quad (\text{IV-8})$$

Since the molecular weight of the styrene monomer is 104.14, this value of  $m_s$  places about 32 monomer units in a statistical segment.

These values may be used to find terminal relaxation times for polymer chains of different molecular weight using the expression

$$\tau_1 = C(N, h^*) \frac{[\eta] M \eta_s}{N_a k T}, \quad (\text{IV-9})$$

where  $C(N, h^*)$  is given by equation (II-165) as

$$C(N, h^*) = \left[ \sum_{p=1}^N \frac{\lambda_1}{\lambda_p} \right]^{-1}. \quad (\text{IV-10})$$

These relaxation times may in turn be compared with those derived for the same set of polystyrene samples using oscillatory flow birefringence data.

As an example of the use of equation (IV-9), the case for  $N=3$  is worked in detail. For the particular curve match under discussion,

$$M = 3 \times 3200 = 9600 \quad (\text{IV-11})$$

for  $N = 3$  segments. The value of  $C(N, h^*)$  for  $h^* = 0.15$  and  $N = 3$  is interpolated from the plot of  $C(N, h^*)$  versus  $N$  for  $h^*$  values of 0.01, 0.1, 0.3, and 0.4 (Figure 6) and is found to be

$$C(3, 0.15) = 0.650. \quad (\text{IV-12})$$

Using the  $\eta_s$  value of 2.23 poises at a temperature of  $25^\circ\text{C}$ ,  $\tau_1$  is directly calculated from equation (IV-9) and is found to be

$$\tau_1 = 6.74 \times 10^{-6} \text{ sec.} \quad (\text{IV-13})$$

The terminal relaxation times  $\tau_1$ , are computed in the above way for the remaining values of  $N$  from 1 to 15 and are shown in Figure 11. The times increase for larger values of  $M$  (and  $N$ ), which seems correct, since the time  $\tau_1$  is associated with the fundamental mode of relaxation of the polymer chain. Thus, longer chains (larger values of  $M$ ) would have longer terminal relaxation times.

A comparison set of relaxation times for polystyrene in Aroclor 1248 may be determined from oscillatory flow birefringence measurements. By comparing theoretical single relaxation time response curves to the low frequency ends of the experimentally measured response curves for the birefringence magnitude and phase angle for each of the polystyrene samples shown in Figure 10, a set of concentration-dependent relaxation times  $\tau_1'(C)$  can be determined. Following the method of Thurston (37), the values for  $\tau_1'(C)$  are assumed to be related to the times  $\tau_1'$  for dilute solutions by the relation

$$\tau_1' = \frac{\tau_1'(C)}{K(C)}, \quad (\text{IV-14})$$

where  $K(c)$  is a concentration factor relating the measured and intrinsic viscosities for each molecular weight sample. Both the times and  $\tau_1$  are shown in Figure 12.

A set of relaxation times  $\tau_1$  can be derived from the  $\tau_1'$  values by the expression

$$\tau_1' = \tau_1 \left( 1 + \frac{\phi}{f} \cdot \frac{1}{N} \cdot \frac{\lambda_1}{\lambda_{1,free}} \right), \quad (\text{IV-15})$$

where  $\phi$  is the coefficient of internal viscosity used by Cerf and Thurston (38). In order to evaluate  $\frac{1}{N} \cdot \frac{\lambda_1}{\lambda_{1,free}}$ , the relation between  $M$  and  $N$  (i.e.,  $m_s$ ) and the value of  $h^*$  must be known. Working with the particular samples of polystyrene under discussion, Thurston has found the approximate value of  $\phi/f$  to be 2.0 (19). A best fit for frequency response curves was obtained for  $h^* = 0.3$  and for a segment molecular weight of 1000. This corresponds to about 10 monomer units per segment. Using these values, the times  $\tau_1'$  in equation (IV-15) may be calculated using the appropriate values of  $\lambda_1$  for the  $N$  value corresponding to a given value of  $M$  and for  $h^* = 0.3$  and 0.0 (i.e., the free-draining case). As an example of the nature of the calculations, the case for  $M = 6000$  is worked in detail. In this case,  $M = 6000$  for  $N = 6$ . The values of  $\lambda_1$  and  $\lambda_{1,free}$  are found from the computed values of  $\lambda_1(N, h^*)$  using the Kirkwood-Riseman expression in equation (II-58). Thus,

$$\lambda_1(6, 0.0) = \lambda_{1,free} = 0.1981, \quad (\text{IV-16})$$

$$\lambda_1(6, 0.3) = 0.2192. \quad (\text{IV-17})$$

Using the value of  $\tau_1'$  for this value of  $M$  as read from Figure 12 and

solving equation (IV-15) for  $\tau_1$  yields

$$\tau_1' = 3.02 \times 10^{-6} \text{ sec}, \quad (\text{IV-18})$$

$$\tau_1 = 2.21 \times 10^{-6} \text{ sec}. \quad (\text{IV-19})$$

Values for  $\tau_1$  for other values of  $N$  from 1 to 15 are found in the same way and are also shown in Figure 12 by a solid line.

These relaxation times can now be compared with those of Figure 11 derived from intrinsic viscosity measurements, which for convenience are also shown in Figure 12 by the dashed line. The values of the two different sets of relaxation times are of the same order of magnitude, differing by a factor of less than two at  $M=4000$  and by about 50 percent at  $M=15,000$ . Both the curves have the same character and appear to approach common values for high molecular weights. Comparison of the two sets is made less revealing by the fact that the times derived from intrinsic viscosity measurements use an estimate of  $N=1$  at  $M=3200$ , while the times from oscillatory flow birefringence data, which, unlike  $[\eta]$  measurements, are made at a finite weight concentration of 3 percent, use an estimate of  $N=1$  at  $M=1000$ .  $m_s$ ,  $h^*$ , and  $\phi/f$  must all be known in order to calculate relaxation times from birefringence measurements, but the variations of these quantities with concentration and molecular weight are unknown. Although the value of  $\phi/f=2.0$  is chosen to fit experimental data, it may be incorrect by  $\pm 50$  percent. Also, the treatment of  $\tau_1'(c)$  and  $\tau_1'$  as being simply related by the factor  $K(c)$  in the same way as the measured and intrinsic viscosities has not been rigorously justified. For these reasons, the times for  $h^*=0.3$  in Figure 12 are not expected to follow those derived from  $[\eta]$  measurements any closer than they do.

Figure 10.  $[\eta]$  Versus  $M$  For Polystyrene in  
Aroclor 1248.



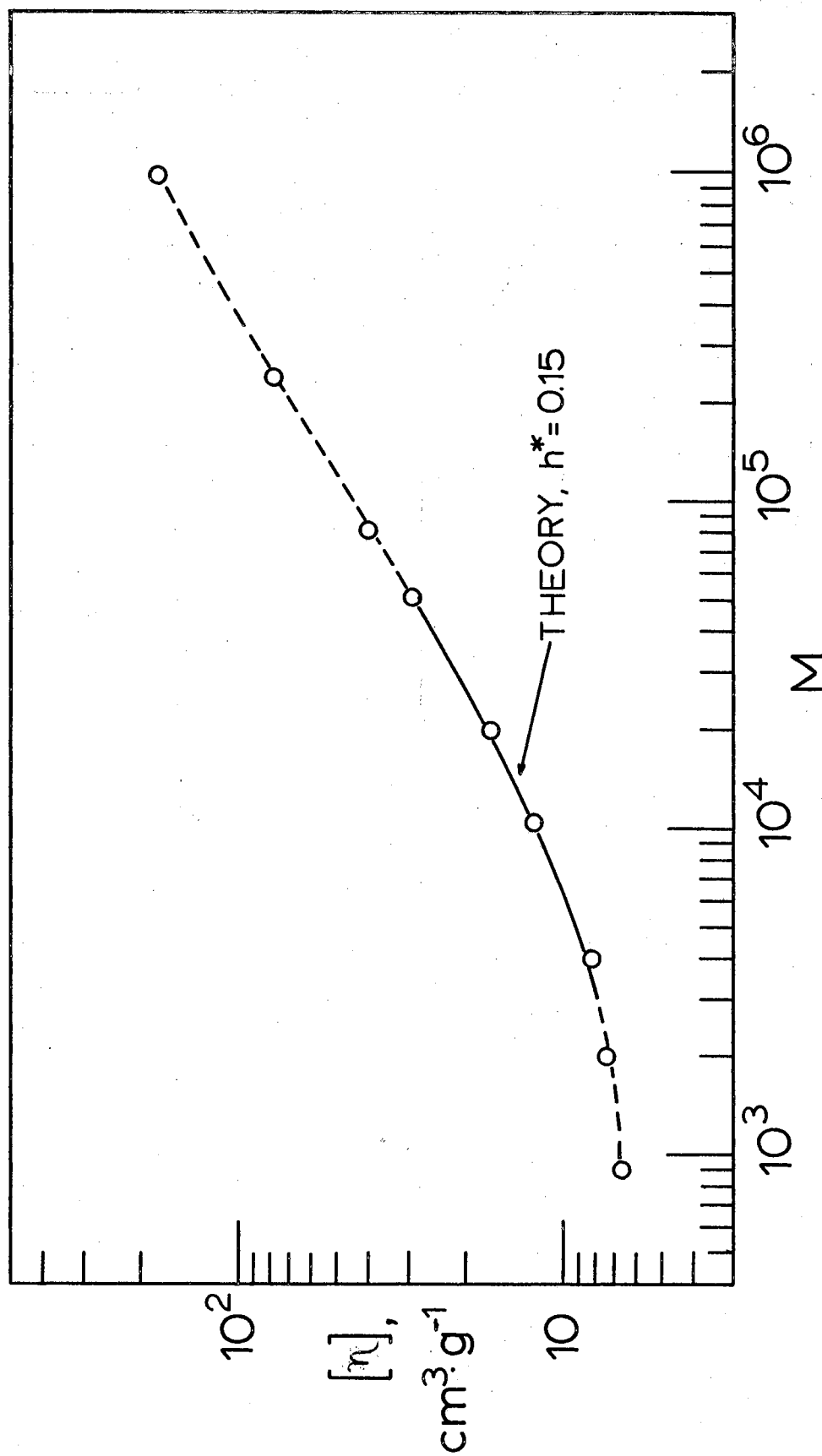


Figure 11.  $\tau_1$  Versus  $M$  Calculated From Intrinsic Viscosity.

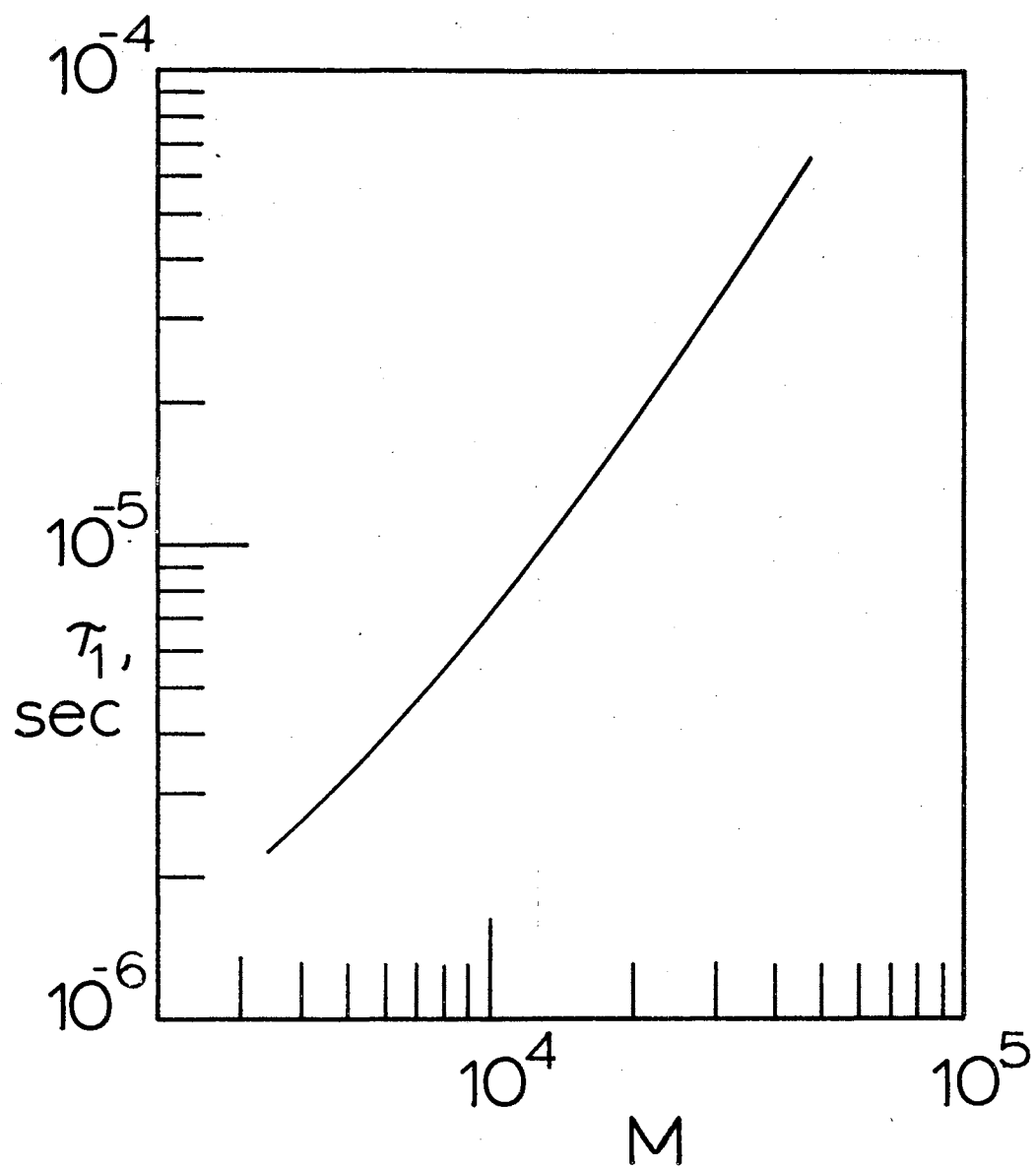
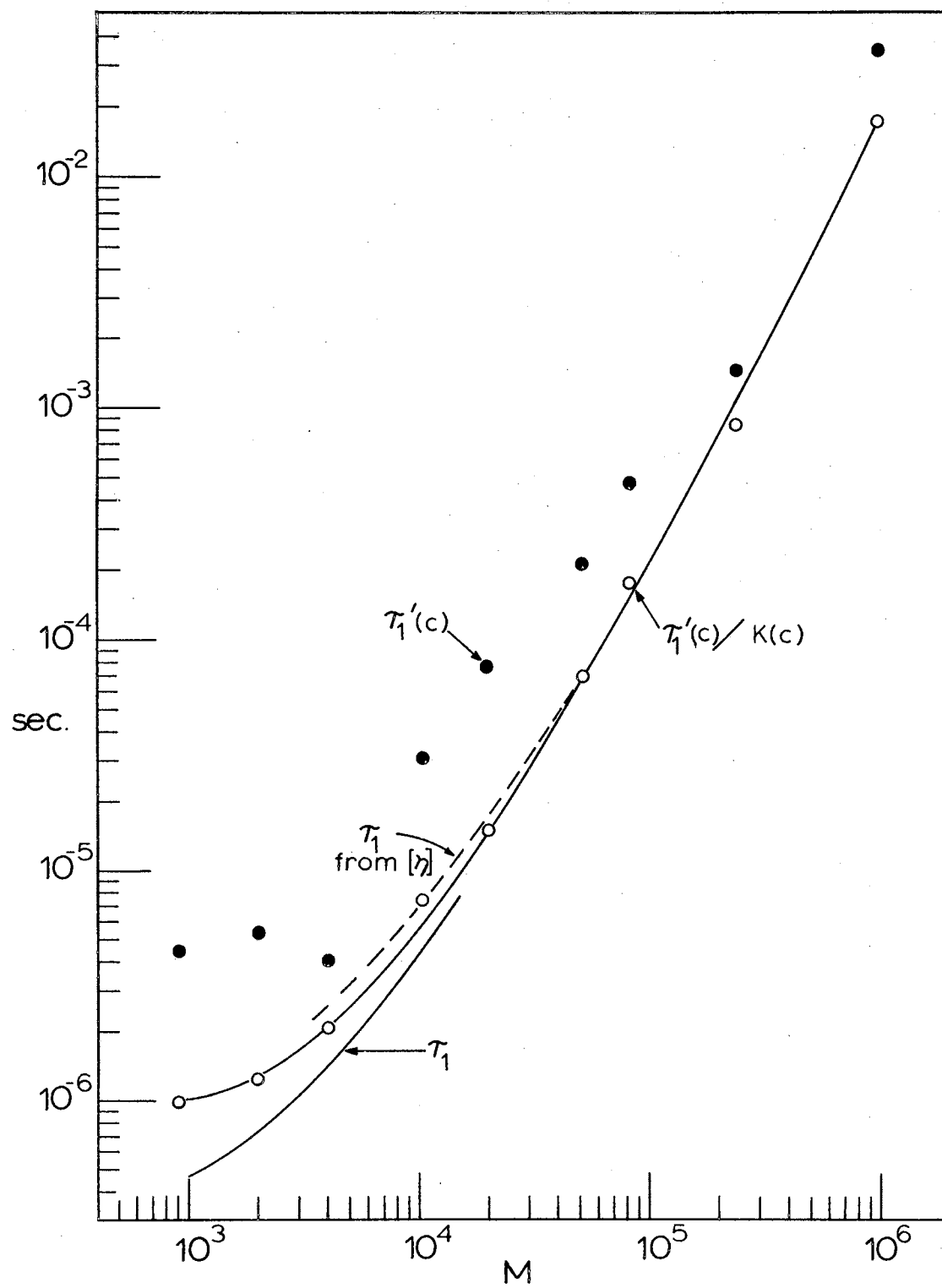


Figure 12. Curves for  $\tau_1'(c)$ ,  $\tau_1'(c)/K(c)$  , and  $\tau_1$  Versus  $M$   
From Oscillatory Flow Birefringence Measure-  
ments.  $\tau_1$  Versus  $M$  From Intrinsic  
Viscosity Measurements.



### Other Intrinsic Viscosity Measurements and Conclusions

Figure 13 presents  $[\eta]$  versus  $M$  data for polystyrene in several solvents taken by Meyerhoff (39) and by Berry (40). In each instance the upward turn of the curve for low molecular weight samples is evident, and has a similar character as the  $\Phi N^{1/2}$  versus  $N$  curves derived from the eigenvalues using the Kirkwood-Riseman expression. The theoretical curves may be matched against the data and yield different values of  $h^*$  for each data series, along with different values for  $m_s$  and  $b$ . At the present time no work exists which simply relates the effect of different solvents upon the parameters  $h^*$ ,  $m_s$ , and  $b$ . One approach to such a theory is a modification of Flory's theory (41) of solvent effects on his equivalent sphere model. Flory's explanation of swelling or compressing the polymer chain coil by placing it in different solvents at different temperatures can be explained within the framework of the Gaussian chain model as a change in the number of monomer units required to make up (on the average) one independently oriented statistical chain element. Placing the polymer in a "good" solvent, i.e., one which tends to increase the end-to-end length of the chain (41, 42), would be accompanied by an increase in  $m_s$  and  $b$  for the particular polymer, while placing the polymer in a "bad" solvent would have the opposite effect. Recent work by Flory and others (43, 44) on the mathematical treatment of polymer chain configurations in terms of the number and size of monomer units in the chain appears to be one starting point to develop a theory to predict changes of  $b$  and  $m_s$ , if not  $h^*$ , from changes in solvent properties.

Figure 14 shows results of  $[\eta]$  versus  $M$  measurements for poly- $\gamma$ -benzyl-L-glutamate in dichloroacetic acid made by Mitchell,

Figure 13.  $[\eta]$  Versus  $M$  for Polystyrene Solutions  
in Benzene (39), Decalin, Dioctylphthalate,  
and Toluene (40).

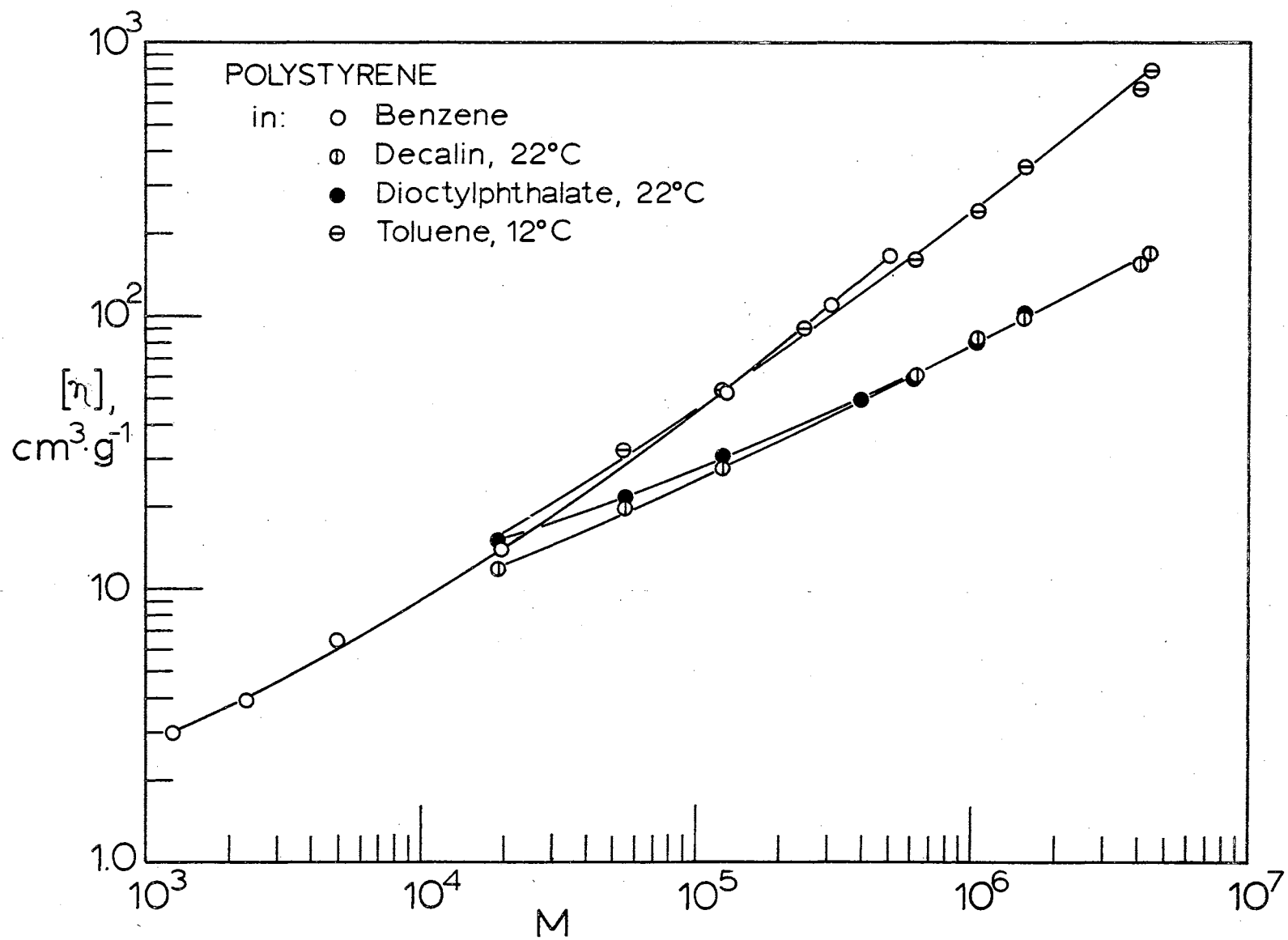
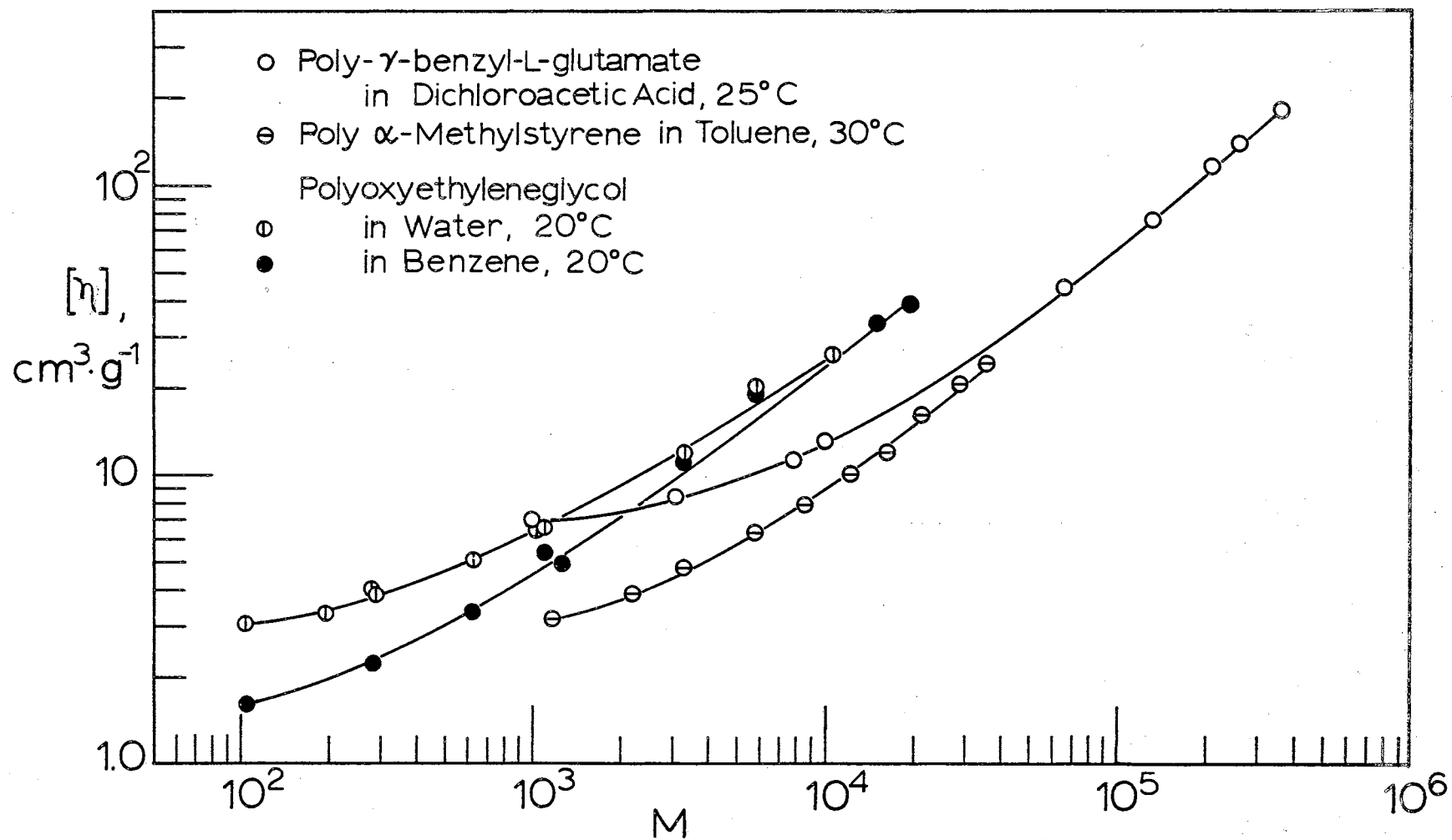




Figure 14.  $[\eta]$  Versus  $M$  for Poly- $\gamma$ -benzyl- L -  
glutamate (45), Poly  $\alpha$ -Methylstyrene (46),  
and Polyoxyethyleneglycol (47).



Woodward, and Doty (45), for poly  $\alpha$ -methylstyrene in toluene made by Cottam, Cowie and Bywater (46) and for polyoxyethyleneglycol in water and benzene by Sadron and Rempp (47). Again the characteristic upward turn of the curves for low molecular weight ranges is evident, and is similar to the character of the  $\phi N^{1/2}$  versus  $N$  curves for low  $N$  using the Kirkwood-Riseman eigenvalues. No calculations for segment mass or length are presented for the polymers shown in Figures 13 and 14, although the curve matching is done in the same manner just described, since there is no extensive data available from oscillatory flow birefringence measurements on the same polymers. This points up the need for sets of good data for intrinsic viscosity and oscillatory flow birefringence over wide ranges of molecular weight for several polymers in different solutions. Without these data sets, there is no independent check of the validity of the values of  $m_s$ ,  $b$ ,  $h^*$  and  $f$  predicted by the present theory, or of the effects of polymer concentration or solvent characteristics upon these parameters.

Within the limitations of the present data, however, the eigenvalues calculated exactly using the Kirkwood-Riseman expression of equation (II-58) are more successful in predicting the behavior of intrinsic viscosity for low molecular weights than are the previously used eigenvalues using the expression due to Pyun and Fixman, which was developed for a model containing a large number of segments. The inclusion of the assumptions that  $N$  is proportional to  $M$  and that  $h^*$  is a constant value for a given polymer-solvent series is successful in predicting the observed character of the molecular weight dependence of the intrinsic viscosity for low molecular weights. The fact that the Kirkwood-Riseman eigenvalues are more successful than the Treloar

eigenvalues in predicting the observed  $[\eta]$ ,  $M$  dependence for low  $M$  indicates that the distributed segment length concept is to be favored over a fixed segment length. The present theory is the only one currently available which can predict the multiple relaxation times observed in frequency response measurements of both oscillatory intrinsic viscosity and flow birefringence experiments.

# BIBLIOGRAPHY

- (1) W. Kuhn and H. Kuhn, J. Coll. Sci. 3, 11 (1948).
- (2) W. Kuhn, Kolloid Z. 68, 2 (1934).
- (3) W. Kuhn and H. Kuhn, Helv. Chim. Acta 26, 1394 (1943).
- (4) W. Kuhn and F. Grun, J. Poly. Sci. 1, 183 (1946).
- (5) H. A. Kramers, J. Chem. Phys. 14, 415 (1946).
- (6) J. J. Hermans, Rec. Trav. Chim. 63, 205 (1944).
- (7) J. G. Kirkwood and J. Riseman, J. Chem. Phys. 16, 565 (1948).
- (8) P. E. Rouse, Jr., J. Chem. Phys. 21, 1272 (1953).
- (9) F. Bueche, J. Chem. Phys. 22, 603 (1954).
- (10) B. H. Zimm, J. Chem. Phys. 24, 269 (1956).
- (11) B. H. Zimm, Rheology, Chapter 1, edited by F. R. Eirich, Academic Press, New York (1960).
- (12) R. Cerf, J. Poly. Sci. 22, 125 (1957).
- (13) R. Cerf, J. Phys. Radium, 19, 122 (1958).
- (14) A. Peterlin, Hydrodynamics of Linear Macromolecules, in International Symposium on Macromolecular Chemistry 2, International Union of Pure and Applied Chemistry, Prague, 1965, Butterworths, London (1966).
- (15) A. Peterlin, J. Poly. Sci. 5, 179 (1967).
- (16) G. B. Thurston and J. L. Schrag, J. Chem. Phys. 45, 3373 (1966).
- (17) G. B. Thurston and A. Peterlin, J. Chem. Phys. 46, 4881 (1967).
- (18) C. W. Pyun and M. Fixman, J. Chem. Phys. 42, 3838 (1965).
- (19) G. B. Thurston and J. L. Schrag, J. Poly. Sci. A2 (to be published July, 1968).

- (20) Yu. Ya. Gotlib and Yu. Ye. Svetlov, Proceedings of the Scientific Conference of the Institute of Macromolecular Compounds, Academy of Science (1965).
- (21) C. Sadron, J. Chim. Phys. 44, 203 (1947).
- (22) C. Sadron, J. Poly. Sci. 3, 241 (1948).
- (23) P. J. Flory, J. Chem. Phys. 17, 214 (1949).
- (24) P. J. Flory and T. G. Fox, J. Am. Chem. Soc. 23, 1904 (1951).
- (25) G. B. Thurston, Polymer 8, 561 (1967).
- (26) A. Peterlin, Polymer 8, 21 (1967).
- (27) M. C. Wang and G. E. Uhlenbeck, Rev. Mod. Phys. 17, 323 (1945), see sections 9 and 10.
- (28) A. Peterlin, J. Chem. Phys. 23, 2464 (1955).
- (29) P. J. Flory and W. R. Krigbaum, J. Chem. Phys. 18, 1086 (1950).
- (30) J. M. Burgers, Second Report on Viscosity and Plasticity of the Amsterdam Academy of Sciences, Koninklijke Nederlandse Akademie Van Wetenschappen, Verhanddingen afd. Naturkunde, section 1, 16 (1938).
- (31) M. V. Volkenstein, Configurational Statistics of Polymeric Chains, Interscience Publishers, New York, Chapter 4 (1963).
- (32) S. Chandrasekhar, Rev. Mod. Phys. 15, 1 (1943).
- (33) Lord Rayleigh, Phil. Mag. 37, 321 (1919).
- (34) F. B. Hildebrand, Methods of Applied Mathematics, Prentice-Hall, Inc., Englewood Cliffs, N. J., Chapter 1 (1963).
- (35) G. B. Thurston, Kolloid Z. 222, 34 (1968).
- (36) C. W. Pyun, Mellon Institute, Carnegie-Mellon University, Pittsburgh, Pa., private communication with G. B. Thurston.
- (37) G. B. Thurston, J. Chem. Phys. 47, 3582 (1967).
- (38) R. Cerf and G. B. Thurston, J. Chim. Phys. 61, 1457 (1964).
- (39) G. Meyerhoff, Zeit. Physik. Chem. N.F. 4, 335 (1955).
- (40) G. C. Berry, J. Chem. Phys. 46, 1338 (1967).
- (41) P. J. Flory, Principles of Polymer Chemistry, Cornell University Press, Ithaca, New York, Chapter 12 (1953).

- (42) W. R. Moore, Progr. Poly. Sci. 1, 43 (1967).
- (43) P. J. Flory and R. L. Jernigan, J. Chem. Phys. 42, 3509 (1965).
- (44) P. J. Flory, Configurational Statistics of Polymer Molecules, Chapter 5 of Proceedings of the Robert A. Welch Foundation Conferences on Chemical Research X. Polymers, Houston, Texas (1967).
- (45) J. C. Mitchell, A. E. Woodward, and Paul Doty, J. Am. Chem. Soc. 79, 3955 (1957).
- (46) B. J. Cottam, J. M. G. Cowie, and S. Bywater, Makromol. Chem. 86, 116 (1965).
- (47) C. Sadron and P. Rempp, J. Poly. Sci. 29, 127 (1958).

VITA

John D. Morrison

Candidate for the Degree of  
Master of Science

Thesis: THE MOLECULAR WEIGHT DEPENDENCE OF INTRINSIC VISCOSITY

Major Field: Physics

Biographical:

Personal Data: Born in Oklahoma City, Oklahoma, August 11, 1944,  
the son of Darius and Lucy Morrison.

Education: Attended grade school in Gracemont, Oklahoma; was  
graduated from Moore High School, Moore, Oklahoma, in 1962;  
received the Bachelor of Science Degree from Oklahoma  
Christian College, with a major in Mathematics, in May, 1965.

Honorary Organizations: Sigma Pi Sigma.